BCS-BEC Crossover

Tristan.W

December 30, 2025

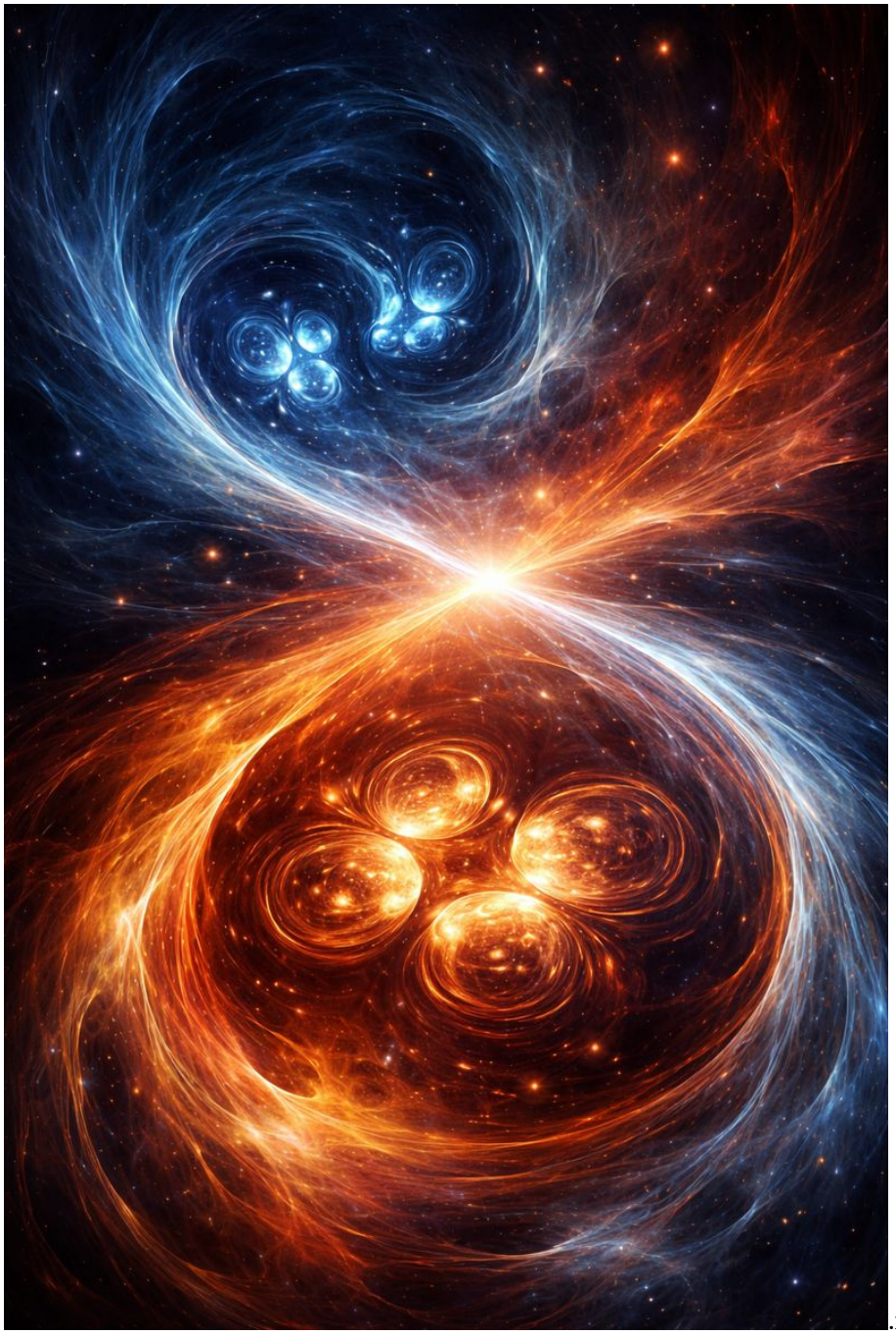 .m;

Contents

1 BCS–BEC crossover: A General Description **3**
- 1.1 BCS limit and weak-coupling pairing (qualitative) . . . 3
- 1.2 BEC limit and real-space bound pairs (qualitative) . . . 4
- 1.3 The BCS wave function as a unifying description: why it can look bosonic . . . 4
- 1.4 Gap equation & Number equation: self-consistent μ and Δ . . . 6

2 BCS limit in detail **6**
- 2.1 Exponentially small gap in $1/(k_F a_s)$ . . . 7
- 2.2 Weak-coupling interpretation of the exponent . . . 7
- 2.3 Momentum distribution and Cooper-pair size . . . 7

3 BEC limit in detail **10**
- 3.1 Basic assumptions and physical meaning . . . 10
- 3.2 Zeroth order in Δ: recovering the two-body bound state . . . 10
- 3.3 Leading order in Δ: interaction effects between molecules . . . 12

4 Excitation and superfluidity **13**
- 4.1 Fermionic excitations: pair breaking . . . 13
- 4.2 Bosonic excitations: phonons and pair COM motion . . . 13
- 4.3 Phenomenological hydrodynamics and sound velocity . . . 13
- 4.4 Critical velocity and robustness of superfluidity . . . 15

5 Transition temperature **16**
- 5.1 Normal state vs superfluid state: what changes above T_c? . . . 16
- 5.2 Landau expansion near a second-order transition . . . 17
- 5.3 Thouless criterion and the BCS limit . . . 17
- 5.4 Why mean-field T_c fails on the BEC side and what fixes it . . . 19
- 5.5 Computational approach: Gaussian fluctuations and NSR . . . 20

6 The unitary regime **21**
- 6.1 Definition and qualitative mean-field ground-state predictions . . . 21
- 6.2 Why theory is difficult: excitations and nonperturbativity . . . 21
- 6.3 Symmetry, possible non-Fermi-liquid behavior, and holographic ideas . . . 21

A Appendix: Solving the coupled gap and number equations for Δ and μ **22**
- A.1 Why the two equations are coupled . . . 22
- A.2 Dimensionless reduction: the only parameter is $-1/(k_F a_s)$ . . . 22
- A.3 Practical solution strategy – A numerical root finding problem . . . 23
- A.4 The BCS limit expansion . . . 25
  - A.4.1 $\tilde{\Delta}$ as a function of λ . . . 25
  - A.4.2 $\tilde{\mu}$ as a function of λ . . . 28
- A.5 The BEC limit expansion . . . 29
- A.6 Physical interpretation of the self-consistent solution . . . 32

1 BCS–BEC crossover: A General Description

The BCS Theory gives a mean field understanding of the *equal-spin, short-range interacting fermion system*. At the heart of this theory lies the BCS Hamiltonian,

$$\hat{H}_{\mathrm{BCS}} = \sum_{\mathbf{k},\sigma} (\epsilon_{\mathbf{k}} - \mu)\hat{c}^{\dagger}_{\mathbf{k}\sigma}\hat{c}_{\mathbf{k}\sigma} - \Delta \sum_{\mathbf{k}} \hat{c}^{\dagger}_{\mathbf{k}\uparrow}\hat{c}^{\dagger}_{-\mathbf{k}\downarrow} - \Delta \sum_{\mathbf{k}} \hat{c}_{-\mathbf{k}\downarrow}\hat{c}_{\mathbf{k}\uparrow} - \frac{V\Delta^2}{g}, \tag{1}$$

which is parametrized by two given parameters, k_F and a_s.

Why k_F and a_s are "given"

k_F is determined by the density of fermions n by

$$n = n_\uparrow + n_\downarrow = \frac{k_F^3}{3\pi^2},$$

, while a_s is defined by the short range interaction,

$$-\frac{1}{g} = -\frac{m}{4\pi\hbar^2 a_s} + \frac{1}{V}\sum_{\mathbf{k}} \frac{1}{2\epsilon_{\mathbf{k}}}. \tag{2}$$

Thus, both of them are free and are tunable in a cold atom experiment.

The Hamiltonian (1) admits two self-consistent equations, namely the number equation (18) and the gap equation (17), which determine the chemical potential μ and the fermionic energy gap Δ once the free parameters are specified. It is customary to introduce a dimensionless parameter

$$\lambda = -\frac{1}{k_F a_s},$$

and the mean-field analysis (i.e., the behavior of μ and Δ) indicates qualitatively distinct physical regimes when this parameter lies in different limits.

For later convenience, we stick to the following settings. We consider a two-component Fermi gas with s-wave scattering length a_s, density n, and Fermi momentum k_F defined by

$$n = n_\uparrow + n_\downarrow = \frac{k_F^3}{3\pi^2}, \qquad E_F = \frac{\hbar^2 k_F^2}{2m}. \tag{3}$$

1.1 BCS limit and weak-coupling pairing (qualitative)

The BCS limit corresponds to

$$a_s < 0, \qquad |k_F a_s| \ll 1 \qquad \left(-\frac{1}{k_F a_s} \gg 1\right). \tag{4}$$

In this regime, the pairing gap Δ is much smaller than the kinetic scale E_F, and pairing mainly reconstructs the many-body state only within a narrow energy window around the Fermi surface.

Momentum-space pairing and the absence of two-body bound states. For $a_s < 0$ in three dimensions, there is no two-body bound state at low energy[1]. The paired state is therefore not a real space binding, but a many-body instability of a Fermi surface (a.k.a. Cooper instability). It is most naturally described as pairing in momentum space, dominated by states near $\epsilon_k \approx \mu \approx E_F$.

[1] It's a well known result. You should feel ashamed if you don't know about it.

In the BCS limit, pairing is weak in the sense that $\Delta/E_F \ll 1$, and only quasiparticles in a thin shell near the Fermi surface are significantly affected. The system retains many fermionic characteristics even though it is not a Fermi liquid in the strict sense[a].

[a] It's not a Fermi Liquid due to the broken $U(1)$ symmetry and gapped excitation near the Fermi Surface.

1.2 BEC limit and real-space bound pairs (qualitative)

On the BEC side,

$$a_s > 0, \qquad k_F a_s \ll 1 \qquad \Big(-\frac{1}{k_F a_s} \ll -1\Big), \tag{5}$$

a stable two-body bound state exists. Unlike a Cooper pair, this bound state is a real-space pair whose typical size scales as $\sim a_s$. One can view it as a diatomic bosonic molecule.

Why the system "loses fermionic character" when the binding energy dominates. When $k_F a_s \ll 1$, the bound-state size is much smaller than the interparticle spacing $\sim 1/k_F$, so the gas is well approximated by a dilute gas of bosonic molecules. Equivalently,

$$a_s \ll \frac{1}{k_F} \quad \Longleftrightarrow \quad \frac{\hbar^2}{m a_s^2} \gg \frac{\hbar^2 k_F^2}{2m} = E_F, \tag{6}$$

i.e., the molecular binding energy scale is much larger than the Fermi energy. In this situation, the relevant low-energy degrees of freedom are molecules (bosons), instead of fermionic quasiparticles with a sharp Fermi surface.

BEC limit: low-energy physics is controlled by tightly bound bosonic molecules of size $\sim a_s$ and binding energy $E_b \sim \frac{\hbar^2}{m a_s^2}$.

1.3 The BCS wave function as a unifying description: why it can look bosonic

A single wave-function family, and Crossover vs Phase Transition. The BCS and BEC limits look very different microscopically, but one can tune $-1/(k_F a_s)$ continuously to connect them. A useful (and operational) characterization of a *crossover* at $T = 0$ is that a single family of many-body wave functions can interpolate smoothly between the two regimes without changing symmetry or topology. For the balanced, spin-singlet superfluid considered here, both limits break the same global $U(1)$ symmetry; thus there is no symmetry obstruction to a smooth interpolation.

BCS state and its exponential representation. The BCS wave function can be written as

$$|\Psi_{\mathrm{BCS}}\rangle \propto \prod_{\boldsymbol{k}} \Big(1 + \frac{v_k}{u_k}\, \hat{c}^\dagger_{k\uparrow} \hat{c}^\dagger_{-k\downarrow}\Big)\, |0\rangle = \exp\Big\{\sum_{\boldsymbol{k}} \frac{v_k}{u_k}\, \hat{c}^\dagger_{k\uparrow} \hat{c}^\dagger_{-k\downarrow}\Big\}\, |0\rangle. \tag{7}$$

The second equality uses the fermionic nilpotency that $\big(\hat{c}^\dagger_{k\sigma}\big)^2 = 0$.

Derivation of the exponential form from fermionic nilpotency

Let $\hat{P}^\dagger_{\boldsymbol{k}} \equiv \hat{c}^\dagger_{k\uparrow} \hat{c}^\dagger_{-k\downarrow}$. Since each mode can be occupied at most once,

$$\big(\hat{P}^\dagger_{\boldsymbol{k}}\big)^2 = 0. \tag{8}$$

Therefore the exponential truncates:

$$\exp\left(\alpha_k \hat{P}_k^\dagger\right) = 1 + \alpha_k \hat{P}_k^\dagger. \tag{9}$$

Moreover, for distinct $\boldsymbol{k} \neq \boldsymbol{k}'$, the pair creators commute:

$$[\hat{P}_k^\dagger, \hat{P}_{k'}^\dagger] = 0, \tag{10}$$

because they are built from disjoint fermion operators. Hence,

$$\prod_k \left(1 + \alpha_k \hat{P}_k^\dagger\right) = \prod_k \exp\left(\alpha_k \hat{P}_k^\dagger\right) = \exp\left(\sum_k \alpha_k \hat{P}_k^\dagger\right), \tag{11}$$

with $\alpha_k = v_k/u_k$. Acting on $|0\rangle$ gives the stated representation.

Introduce

$$\tilde{g}_k \equiv \frac{v_k}{u_k}, \qquad \mathcal{A} \equiv \sum_k |\tilde{g}_k|^2, \qquad g_k \equiv \frac{\tilde{g}_k}{\sqrt{\mathcal{A}}}. \tag{12}$$

Define a (composite) Cooper-pair creation operator

$$\hat{b}^\dagger \equiv \sum_k g_k \, \hat{c}_{k\uparrow}^\dagger \hat{c}_{-k\downarrow}^\dagger. \tag{13}$$

Then the BCS state can be viewed as

$$|\Psi_{\mathrm{BCS}}\rangle \propto \exp\left(\sqrt{\mathcal{A}}\, \hat{b}^\dagger\right)|0\rangle, \tag{14}$$

suggesting a coherent-state-like structure if $\hat{b}$ behaves approximately bosonically.

When does $\hat{b}$ behave like a boson?. A direct calculation gives

$$[\hat{b}, \hat{b}^\dagger] = \sum_k |g_k|^2 \left(1 - \hat{n}_{k\uparrow} - \hat{n}_{-k\downarrow}\right). \tag{15}$$

When the occupation numbers $\hat{n}_{k\uparrow}$ and $\hat{n}_{-k\downarrow}$ can be neglected (e.g., in the dilute molecular regime where fermions are mostly locked into tightly bound pairs), the right-hand side approaches 1, and $\hat{b}$ approximately obeys bosonic commutation relations. In the same regime, the real-space pair wave function becomes tightly bound with size $\sim a_s$.

Cooper-pair wave function: momentum space vs real space

Relative vs center-of-mass motion.
The pair creation operator

$$\hat{b}^\dagger = \sum_k g_k \, \hat{c}_{k\uparrow}^\dagger \hat{c}_{-k\downarrow}^\dagger$$

creates two fermions with opposite momenta $\boldsymbol{k}$ and $-\boldsymbol{k}$. As a result, the center-of-mass (COM) momentum of the pair vanishes, while $\boldsymbol{k}$ labels the *relative momentum* within the pair. Therefore, the coefficient g_k specifies how strongly a given relative-momentum channel $\mathbf{k}$ contributes to the Cooper pair.

Physical meaning of g_k. Since $\hat{b}^\dagger$ is a coherent superposition of fermion pairs with different relative momenta, $|g_k|^2$ directly measures the weight of relative momentum $\boldsymbol{k}$ in the internal structure of the Cooper pair. In this sense, g_k plays the role of a *momentum-space wave function* for the relative motion of the two fermions.

Real-space relative wave function. To expose the spatial structure of the pair, we introduce the real-space field operator

$$\psi_\sigma^\dagger(\boldsymbol{r}) = \frac{1}{\sqrt{V}} \sum_{\boldsymbol{k}} e^{-i\boldsymbol{k}\cdot\boldsymbol{r}} \hat{c}_{\boldsymbol{k}\sigma}^\dagger.$$

A zero-COM pair can then be created in real space as

$$\hat{b}^\dagger \propto \int d^3R \int d^3r\, \psi(\boldsymbol{r})\, \psi_\uparrow^\dagger\left(\boldsymbol{R} + \frac{\boldsymbol{r}}{2}\right) \psi_\downarrow^\dagger\left(\boldsymbol{R} - \frac{\boldsymbol{r}}{2}\right),$$

where $\boldsymbol{R}$ and $\boldsymbol{r}$ denote the COM and relative coordinates, respectively. Matching this expression with the momentum-space definition yields

$$\psi(\boldsymbol{r}) = \frac{1}{\sqrt{(2\pi)^3}} \int d^3k\, g_{\boldsymbol{k}}\, e^{i\boldsymbol{k}\cdot\boldsymbol{r}}. \tag{16}$$

Physical meaning of $\psi(\boldsymbol{r})$. The function $\psi(\boldsymbol{r})$ is the Fourier transform of $g_{\boldsymbol{k}}$ and therefore represents the *relative-coordinate wave function* of the Cooper pair. It encodes the typical spatial separation between the two fermions and thus characterizes the size and real-space structure of the pair. In the BEC regime, $\psi(\boldsymbol{r})$ is strongly localized with size set by the scattering length a_s, whereas in the BCS regime it extends over a much larger coherence length.

1.4 Gap equation & Number equation: self-consistent μ and Δ

Why μ is the compass needle of BCS-BEC Crossover.

The chemical potential μ changes qualitatively across the crossover: $\mu \approx E_F$ in the BCS limit, while $\mu \approx -E_b/2$ in the BEC limit with $E_b \sim \hbar^2/(ma_s^2)$. Also, Δ must be obtained by solving the gap equation together with number conservation.

Standard mean-field equations. The mean-field gap equation can be written in a renormalized form as

$$-\frac{m}{4\pi\hbar^2 a_s} = \frac{1}{V} \sum_{\boldsymbol{k}} \left(\frac{1}{2E_k} - \frac{1}{2\epsilon_k} \right), \tag{17}$$

and the number equation[2]

$$n_\sigma = \frac{1}{V} \sum_{\mathbf{k}} n_{\mathbf{k}\sigma} = \frac{1}{2V} \sum_{\boldsymbol{k}} \left(1 - \frac{\epsilon_k - \mu}{E_k} \right). \tag{18}$$

Solving (17) and (18) self-consistently yields Δ/E_F and μ/E_F as functions of $-1/(k_F a_s)$.

Across the crossover, Δ and μ are not independent: the physically meaningful prediction is obtained only from the *simultaneous* solution of the renormalized gap equation (17) and the number equation (18).

2 BCS limit in detail

By systematically solving and analyzing the gap equation (17) together with the number equation (18), we can understand the behavior of the BCS Mean-Field theory in detail. In

[2]Here is a common confusion due to the abuse of notation. $n_\sigma = \frac{1}{2}n = \frac{k_F^3}{6\pi^3}$ is the number density of a spin component, while $n_{\mathbf{k}\sigma} = c_{\mathbf{k}\sigma}^\dagger c_{\mathbf{k}\sigma}$ is the number operator of the quantum state at $(\mathbf{k}, \sigma)$.

this chapter, we present the main results of the BCS limit, while the technical derivations are deferred to Appendix A.

2.1 Exponentially small gap in $1/(k_F a_s)$

BCS assumptions and leading approximation. In the BCS limit, $\Delta \ll \mu$, and the number equation reduces to that of a free Fermi gas, giving

$$\mu \simeq E_F. \tag{19}$$

Substituting $\mu = E_F$ into the gap equation yields the approximate solution

$$\Delta = \frac{8E_F}{e^2} \exp\left\{\frac{\pi}{2k_F a_s}\right\}. \tag{20}$$

For $a_s < 0$, the exponent is negative and Δ/E_F is exponentially small.

> **BCS limit**: Δ/E_F is exponentially small in $1/(k_F a_s)$.
> The smallness of Δ is the precise quantitative statement behind "weak-coupling pairing".

2.2 Weak-coupling interpretation of the exponent

Density of states and effective interaction. The exponent can be rewritten as

$$\frac{\pi}{2k_F a_s} = \frac{1}{D(E_F)U} \tag{21}$$

where[3]

$$D(E_F) = \frac{mk_F}{2\hbar^2\pi^2} \tag{22}$$

is the density of states at the Fermi energy, and

$$U = \frac{4\pi\hbar^2 a_s}{m} \tag{23}$$

is the low-energy contact interaction strength (after renormalization to a_s).

> This form emphasizes that only states near E_F matter at leading order: the pairng instability (*i.e. the gap* Δ) is controlled by $D(E_F)$ and the effective coupling U.

2.3 Momentum distribution and Cooper-pair size

■ **Momentum distribution: Energy window $\sim \Delta$ around the Fermi surface.**
In mean-field theory at $T = 0$,

$$n_{k\sigma} \equiv v_k^2 = \frac{1}{2}\left(1 - \frac{\epsilon_k - \mu}{E_k}\right). \tag{24}$$

[3]Note that $D(E_F) = \frac{dN}{dE}\Big|_{E=E_F} = \frac{dN/dk}{dE/dk}\Big|_{k=k_F}$. Use the relation $\frac{dN}{dk} = \frac{V}{(2\pi)^3} 4\pi k^2$, $\frac{dE}{dk} = \frac{\hbar^2 k}{m}$ and you get the result. The difference of V is a convention whether you talk about the DOS in the phase space or in the momentum space. You should feel ashamed if you forget how to calculate $D(E_F)$.

Note that $\xi_k \equiv \epsilon_k - \mu$ and $E_k = \sqrt{\xi_k^2 + \Delta^2}$, so $n_{k\sigma}$ can be expressed as a function of (ξ_k/Δ) [4]:

$$n_{k\sigma} = v_k^2 = \frac{1}{2}\left(1 - \frac{\xi_k/\Delta}{\sqrt{(\xi_k/\Delta)^2 + 1}}\right). \tag{25}$$

The behavior of (25) is shown below in Fig 1.

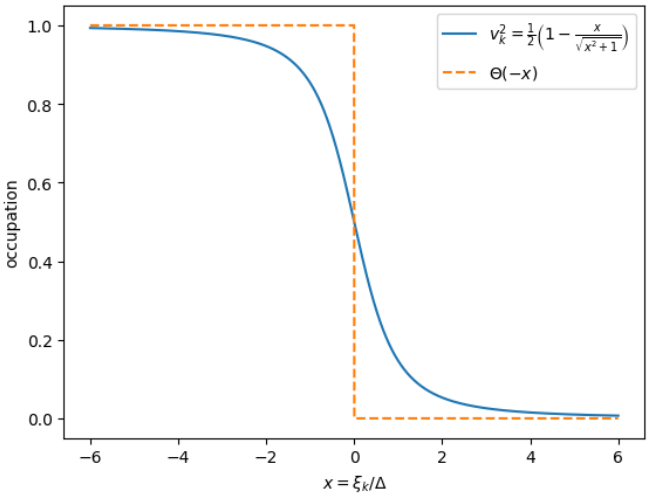

Figure 1: BEC momentum distribution vs step-function

Thus, $n_{k\sigma}$ deviates significantly from a step function only for $|\epsilon_k - \mu| \lesssim \Delta$. Hence the pairing-induced reconstruction of the momentum distribution is confined to an small energy shell of width $\sim \Delta$ around the Fermi surface.

■ **Cooper-pair size: Momentum space and Real space estimation.**

We first estimate the Cooper-pair wave function in momentum space, defined in (12)
Here u_k and v_k are the usual BCS coherence factors,

$$u_k^2 = \frac{1}{2}\left(1 + \frac{\xi_k}{E_k}\right), \qquad v_k^2 = \frac{1}{2}\left(1 - \frac{\xi_k}{E_k}\right),$$

with $\xi_k = \epsilon_k - \mu$ and $E_k = \sqrt{\xi_k^2 + \Delta^2}$. A simple algebraic manipulation gives the closed form

$$\tilde{g}_k = \frac{v_k}{u_k} = \sqrt{\frac{E_k - \xi_k}{E_k + \xi_k}} = \frac{\Delta}{E_k + \xi_k}. \tag{26}$$

In terms of the dimensionless variables $x = k/k_F$, $\tilde{\mu} = \mu/E_F$, and $\tilde{\Delta} = \Delta/E_F$, this can be written as

$$\tilde{g}(x) = \frac{\tilde{\Delta}}{\sqrt{(x^2 - \tilde{\mu})^2 + \tilde{\Delta}^2} + (x^2 - \tilde{\mu})}. \tag{27}$$

This expression makes the qualitative behavior of g_k transparent. As a function of $x = k/k_F$, $\tilde{g}_k$ is a smooth, strictly monotonic decreasing function:

- For $x \to 0$, one has $\tilde{g}_k \sim \frac{2\tilde{\mu}}{\tilde{\Delta}} \gg 1$
- For $x \to \infty$, one has $\tilde{g}_k \sim \frac{\tilde{\Delta}}{2x^2} \to 0$

[4] Note that $\mu \sim E_F$ in BCS limit, so $\xi_k \equiv \epsilon_k - \mu$ measures the deviation from the Fermi Surface. Consequently, ξ_k/Δ measures whether the momentum k lies within the Δ window.

- Moreover, $\tilde{g}_k = 1$ precisely at $x = \tilde{\mu}$

Thus $\tilde{g}_k$ exhibits a single, monotonic crossover from large to small values, centered around momenta of order k_F.

For a given coupling $\lambda = -1/(k_F a_s)$, the self-consistent values of $\tilde{\Delta}$ and $\tilde{\mu}$ are obtained by solving the mean-field gap and number equations, see Appendix 1. Substituting these into the above expression (27) yields the full momentum dependence of g_k, which can be evaluated numerically[5]. Representative results are shown in Fig 2a.

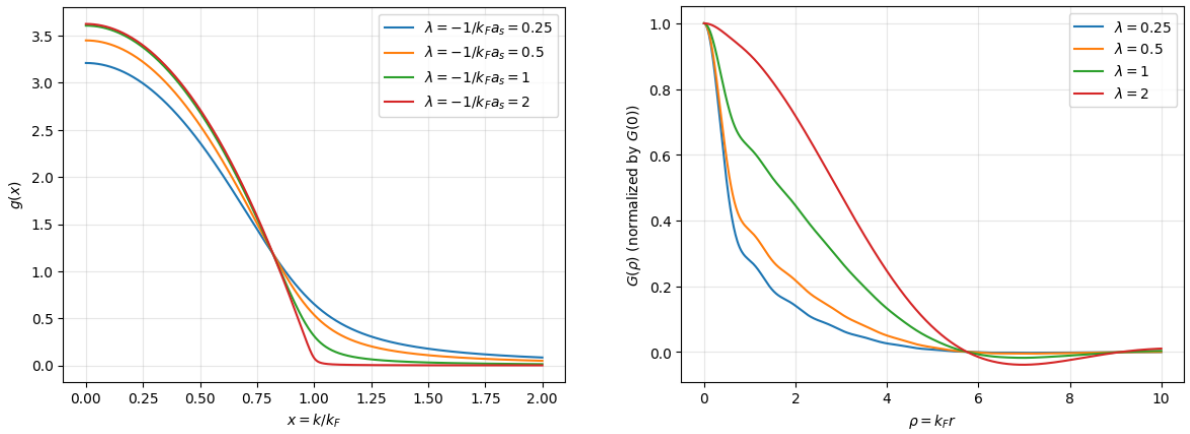

(a) g_k vs k/k_F (b) G_r vs $k_F r$

Figure 2: Cooper-pair size in the BCS limit

One clearly sees that in the BCS limit ($\lambda = -1/k_F a_s \to +\infty$) the momentum-space pair wave function has a characteristic width of order k_F, reflecting the fact that the crossover of g_k occurs when $\epsilon_k \sim \mu$.

Finally, the real-space pair wave function is obtained by Fourier transformation,

$$\psi(\boldsymbol{r}) = \frac{1}{\sqrt{(2\pi)^3}} \int d^3k \, g_{\boldsymbol{k}} \, e^{i\boldsymbol{k}\cdot\boldsymbol{r}}.$$

Since g_k is a smooth function with its dominant variation on the momentum scale $k \sim k_F$, its Fourier transform necessarily exhibits oscillations with wave vector k_F and a characteristic spatial scale of order $\xi_{\text{pair}} \sim 1/k_F$. This provides a simple order-of-magnitude estimate for the size of a Cooper pair in the weak-coupling BCS regime. A numerical result is shown in Fig 2b,where $\xi_{\text{pair}} \simeq 5.5/k_F$.

Analog of a Gaussian Wave Packet

The momentum-space Cooper-pair wave function g_k exhibits a smooth, single-peaked profile with a characteristic crossover scale in k, which makes it qualitatively analogous to a Gaussian wave packet. Although g_k is not exactly Gaussian, many of its qualitative features— in particular the relation between momentum-space width and real-space extent— are the same. It is therefore instructive to briefly recall the Fourier transform properties of a Gaussian wave packet.

Consider a normalized Gaussian wave packet in momentum space,

$$\phi(k) = \frac{1}{(\pi\sigma_k^2)^{1/4}} \exp\left[-\frac{(k-k_0)^2}{2\sigma_k^2}\right],$$

[5]To evaluate the normalized g_k, one need to evaluate$\mathcal{A} \equiv \sum_k |\tilde{g}_k|^2$. A practical way is to turn the summation to an integral and set a reasonable truncation.

where k_0 is the central momentum and σ_k characterizes the momentum-space width. Its Fourier transform gives the real-space wave function

$$\phi(x) = \frac{(\sigma_k)^{1/2}}{(\pi)^{1/4}} \exp\left[-\frac{\sigma_k^2 x^2}{2}\right] e^{ik_0 x}.$$

The key feature is the inverse relation between the widths:

$$\sigma_x \sim \frac{1}{\sigma_k},$$

so that localization in momentum space implies delocalization in real space, and vice versa.

3 BEC limit in detail

By systematically solving and analyzing the gap equation (17) together with the number equation (18), we can understand the behavior of the BCS Mean-Field theory in detail. In this chapter, we present the main results of the BEC limit, while the technical derivations are deferred to Appendix A.

3.1 Basic assumptions and physical meaning

Negative chemical potential and small-Δ expansion. In the BEC limit the chemical potential becomes negative. Assuming [6]

$$\mu < 0, \qquad (-\mu) \gg \Delta, \tag{28}$$

one has $|\epsilon_k - \mu| \gg \Delta$, enabling a controlled expansion in Δ. Physically, $-\mu$ sets the binding-energy scale of tightly bound molecules, while Δ captures residual many-body coherence effects.

3.2 Zeroth order in Δ: recovering the two-body bound state

Gap equation reduces to the two-body bound state equation.

To zeroth order in Δ, the gap equation becomes

$$-\frac{m}{4\pi\hbar^2 a_s} = \sum_{\boldsymbol{k}} \left(\frac{1}{2\epsilon_k - 2\mu} - \frac{1}{2\epsilon_k} \right). \tag{29}$$

By identifying 2μ with the two-body energy E, one sees that (29) reproduces the two-body bound-state condition, leading to

$$\frac{\mu}{E_F} = -\left(\frac{1}{k_F a_s}\right)^2. \tag{30}$$

This matches the expectation that μ equals half the two-body binding energy.

■ **Disappearance of the Fermi surface, and the validity of bosonic commutator.**

In the BEC limit, $\xi_k = \epsilon_k - \mu \geq -\mu \gg \Delta$, so $E_k = \sqrt{\xi_k^2 + \Delta^2} \simeq \xi_k + \frac{\Delta^2}{2\xi_k}$. Plugging in the expression of v_k^2:

$$v_k^2 = \frac{1}{2}\left(1 - \frac{\xi_k}{E_k}\right) \simeq \frac{1}{2}\left(1 - \frac{\xi_k}{\xi_k + \frac{\Delta^2}{2\xi_k}}\right) \simeq \frac{\Delta^2}{4\xi_k^2}.$$

[6] The reason for this assumption is explained in Appendix A.

With $\xi_k \gg \Delta$, one finds $v_k^2 \approx 0$ and thus $n_{k\sigma} \approx 0$.

Then the commutator (15) reduces to $[\hat{b}, \hat{b}^\dagger] \approx 1$, and $\hat{b}$ behaves bosonically. In this regime the momentum distribution becomes broad and smooth, with no sharp Fermi-surface feature.

One can also numerically investigate $n_{k\sigma}$. First, numerically obtain the value of Δ and μ at different values of λ, using the technique introduced in Appendix A. Then plug in the expression of $n_{k\sigma}$ (24), and plot. The result is shown in Fig 3, where one can see that there is no "Fermi Surface" and the number density goes to zero at BEC limit.

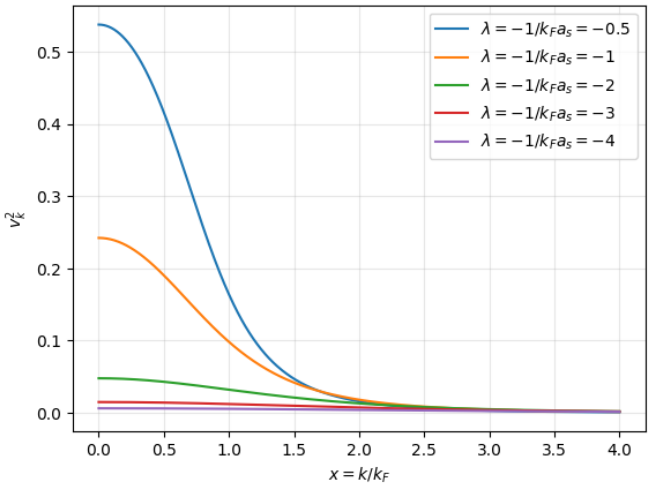

Figure 3: n_k vs k/k_F

■ **Cooper-pair size: Momentum space and Real space estimation..**

We first estimate the momentum space cooper pair wavefunction. See (26). Using the BEC limit relation $\Delta \ll |\mu| < \xi_k$, one can take $E_k = \sqrt{\xi_k^2 + \Delta^2} \simeq \xi_k$. So:

$$\begin{aligned} \tilde{g}_k &= \frac{v_k}{u_k} = \frac{\Delta}{E_k + \xi_k} \\ &\simeq \frac{\Delta}{2\epsilon_k - 2\mu} = \frac{\tilde{\Delta}}{2x^2 - 2\tilde{\mu}} \qquad (x \equiv k/k_F) \\ &= \frac{m\Delta}{\hbar^2} \frac{1}{k^2 + (1/a_s)^2}. \end{aligned} \tag{31}$$

The typical spread of momentum space pairing wavefunction (31) can be estimated as $1/a_s$.

One can also try numerics without doing any approximation. For a given coupling $\lambda = -1/(k_F a_s)$, the self-consistent values of $\tilde{\Delta}$ and $\tilde{\mu}$ are obtained by solving the mean-field gap and number equations, see Appendix A. Substituting these into the exact $\tilde{g}_k$ fomula (31) yields Fig 4a.

Then we turn to the real space Cooper pair wavefunction.

$$\psi(\boldsymbol{r}) = \frac{1}{\sqrt{(2\pi)^3}} \int d^3k \, g_{\boldsymbol{k}} \, e^{i\boldsymbol{k}\cdot\boldsymbol{r}}.$$

A well-known fact[7] is that:

$$\int \frac{d^3k}{(2\pi)^3} \frac{e^{i\boldsymbol{k}\cdot\boldsymbol{r}}}{k^2 + \kappa^2} = \frac{1}{4\pi} \frac{e^{-\kappa r}}{r},$$

so $\psi(r) \propto \frac{e^{-r/a_s}}{r}$ and the typical binding state size is a_s, as expected. A numerical result is shown in Fig 4b.

[7] If you don't know about this, you should apologize to your QFT instructor and Prof. Steven Weinberg.

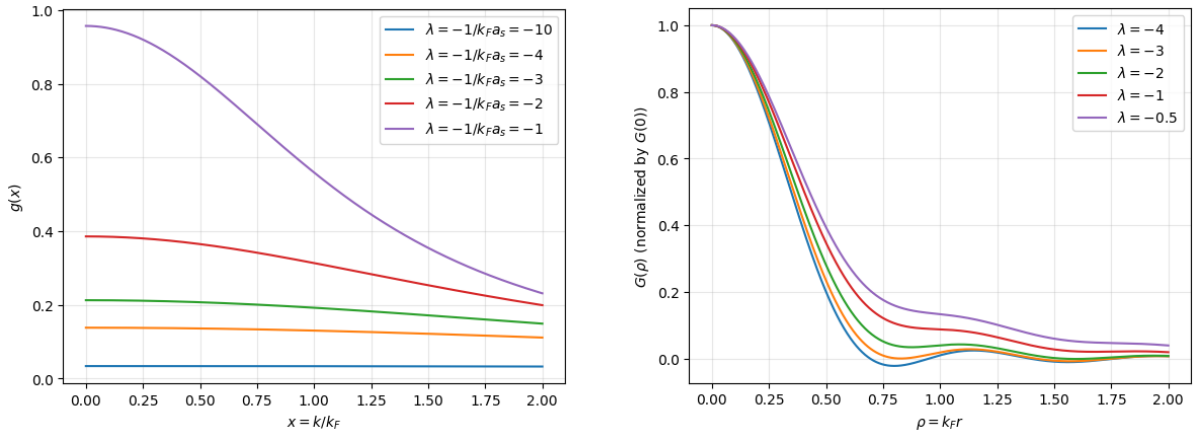

(a) g_k vs k/k_F

(b) G_r vs $k_F r$

Figure 4: Cooper-pair size in the BEC limit

3.3 Leading order in Δ: interaction effects between molecules

Number equation fixes the scaling of Δ.

To leading order in Δ, the number equation yields

$$\frac{16}{3\pi} = \left(\frac{\Delta}{E_F}\right)^2 \sqrt{\frac{E_F}{-\mu}}. \tag{32}$$

Using (30), one obtains

$$\Delta = \frac{4E_F}{\sqrt{3\pi k_F a_s}}, \qquad \frac{\Delta}{-\mu} \sim (k_F a_s)^{3/2} \ll 1, \tag{33}$$

justifying the small-Δ expansion.

First correction to μ and molecular equation of state.

Including the leading correction, the chemical potential becomes

$$\frac{\mu}{E_F} = -\frac{1}{(k_F a_s)^2} + \frac{2k_F a_s}{3\pi}. \tag{34}$$

Introduce the molecular chemical potential $\mu_m \equiv 2\mu$. Then one may write

$$\mu_m = -\frac{\hbar^2}{m a_s^2} + \frac{4\pi\hbar^2(2a_s)}{(2m)}\, n_m, \tag{35}$$

where $n_m = n_\uparrow = n_\downarrow = k_F^3/(6\pi^2)$. The first term is the binding energy and the second term reflects repulsive molecule–molecule interaction, suggesting an effective molecule–molecule scattering length

$$a_m = 2a_s \tag{36}$$

at this mean-field level.

More accurate value and physical origin of repulsion. A more rigorous four-body calculation yields $a_m = 0.6a_s$. Despite the coefficient difference, the key feature $a_m \propto a_s$ is captured: repulsion originates from the composite nature of molecules and the Pauli exclusion principle, which becomes important when molecules approach within a distance comparable to their size $\sim a_s$.

BEC limit: $\mu \approx -E_b/2$ at zeroth order, while the leading correction encodes repulsive molecule–molecule interactions and implies $a_m \propto a_s$.

4 Excitation and superfluidity

4.1 Fermionic excitations: pair breaking

Breaking a Cooper pair creates singly occupied fermionic modes; thus it is called a *fermionic excitation*. In mean-field theory the excitation gap depends on μ:

- $\mu > 0$. The minimum excitation gap occurs at $\epsilon_k = \mu$ and equals Δ.
- $\mu < 0$. The minimum occurs at $k = 0$ and equals $\sqrt{\mu^2 + \Delta^2}$.

From the behavior of μ and Δ across the crossover, the fermionic excitation gap increases monotonically from the BCS limit to the BEC limit.

Why $\Delta E_{\text{fermionic}}$ increases monotonically from the BCS limit to the BEC limit?

The reason is simple. When λ goes from a large positive value(BCS limit) to zero(Unitary), Δ increases. When it goes from zero(Unitary) to a large negative value(BEC limit), $|\mu|$ and Δ both increases.

4.2 Bosonic excitations: phonons and pair COM motion

A Bose condensate supports a linear, gapless phonon mode $\omega = ck$, corresponding to long-wavelength density/phase oscillations. In the BEC regime, it represents finite-momentum motion of diatomic moleculesm, which is the motion of the molecule center of mass. The corresponding bosonic mode should also exist in the BCS regime, describing finite center of mass motion of Cooper pairs.

Why BCS mean field alone does not produce this mode. The mean-field Hamiltonian used to derive the BCS quasiparticles typically keeps only the zero center-of-mass momentum pairing channel:

$$\sum_{\mathbf{k}\mathbf{k}'\mathbf{q}} \hat{c}^\dagger_{\mathbf{k}+\frac{\mathbf{q}}{2}\uparrow} \hat{c}^\dagger_{-\mathbf{k}+\frac{\mathbf{q}}{2}\downarrow} \hat{c}_{-\mathbf{k}'+\frac{\mathbf{q}}{2}\downarrow} \hat{c}_{\mathbf{k}'+\frac{\mathbf{q}}{2}\uparrow} \longrightarrow \sum_{\mathbf{k}\mathbf{k}'} \hat{c}^\dagger_{\mathbf{k}\uparrow} \hat{c}^\dagger_{-\mathbf{k}\downarrow} \hat{c}_{-\mathbf{k}'\downarrow} \hat{c}_{\mathbf{k}'\uparrow} \qquad \text{(keeping only } q = 0 \text{ channel)} \tag{37}$$

As a result, collective modes associated with finite COM pair fluctuations are not automatically captured at that level; one must incorporate fluctuations beyond static mean field.

4.3 Phenomenological hydrodynamics and sound velocity

A phenomenological hydrodynamic approach gives

$$\frac{\partial^2 \delta n}{\partial t^2} = \frac{1}{m} \nabla \left[n \nabla \left(\frac{\partial \mu}{\partial n} \delta n \right) \right], \tag{38}$$

leading to a low-energy phonon dispersion $\omega = ck$ with

$$mc^2 = n \frac{\partial \mu}{\partial n}. \tag{39}$$

BCS and BEC limiting forms.

- **BCS side.** Taking $\mu \approx E_F$, the sound velocity saturates to the noninteracting Fermi-gas value $c \to v_F/\sqrt{3}$.

BCS limit: deriving $c = v_F/\sqrt{3}$ from $mc^2 = n\,\partial\mu/\partial n$

In the weak-coupling BCS regime the equation of state is essentially that of a free Fermi gas, so we take $\mu \simeq E_F$. In three dimensions,

$$k_F = (3\pi^2 n)^{1/3}, \qquad E_F = \frac{\hbar^2 k_F^2}{2m} = \frac{\hbar^2}{2m}(3\pi^2 n)^{2/3}.$$

Therefore

$$\frac{\partial \mu}{\partial n} \simeq \frac{\partial E_F}{\partial n} = \frac{2}{3}\frac{E_F}{n}.$$

Plugging this into the hydrodynamic relation (39) gives

$$mc^2 = n\frac{\partial \mu}{\partial n} \simeq n \cdot \frac{2}{3}\frac{E_F}{n} = \frac{2}{3}E_F,$$

hence

$$c^2 = \frac{2E_F}{3m} = \frac{1}{3}\left(\frac{2E_F}{m}\right) = \frac{v_F^2}{3}, \qquad v_F \equiv \frac{\hbar k_F}{m}.$$

So the sound velocity approaches $c = v_F/\sqrt{3}$ up to weak interaction corrections.

■ **BEC side.** With $\mu = \mu_m/2$ and μ_m as in (35), one finds

$$c = \frac{\sqrt{4\pi\hbar^2 a_m n_m}}{2m}, \tag{40}$$

which increases as a_s increases on the $a_s > 0$ side (through $a_m \propto a_s$).

BEC limit: deriving $c = \sqrt{4\pi\hbar^2 a_m n_m/(2m)^2}$

In the BEC regime the low-energy degrees of freedom are bosonic molecules with mass $m_B = 2m$ and density $n_m = n/2$. Their mean-field chemical potential is

$$\mu_m = g_m n_m, \qquad g_m = \frac{4\pi\hbar^2 a_m}{m_B} = \frac{4\pi\hbar^2 a_m}{2m}.$$

The fermionic chemical potential per atom is related by $\mu = \mu_m/2$. Using $n = 2n_m$,

$$\frac{\partial \mu}{\partial n} = \frac{\partial(\mu_m/2)}{\partial(2n_m)} = \frac{1}{4}\frac{\partial \mu_m}{\partial n_m} = \frac{1}{4}g_m.$$

Then (39) gives

$$mc^2 = n\frac{\partial \mu}{\partial n} = (2n_m)\cdot\frac{1}{4}g_m = \frac{n_m g_m}{2} = \frac{\mu_m}{2},$$

so

$$c^2 = \frac{n_m g_m}{2m} = \frac{n_m}{2m}\cdot\frac{4\pi\hbar^2 a_m}{2m} = \frac{4\pi\hbar^2 a_m n_m}{(2m)^2}.$$

Equivalently, writing it in the compact form used in the text,

$$c = \frac{\sqrt{4\pi\hbar^2 a_m n_m}}{2m}, \tag{41}$$

where the factor of $2m$ reflects the molecular mass scale; in practice one should keep track consistently of whether the hydrodynamic mass parameter is taken per atom (m) or per molecule ($2m$).

A fully controlled derivation across the entire crossover requires going beyond mean field, e.g. using the random phase approximation (RPA), which also addresses how the sound velocity evolves through the unitary regime.

4.4 Critical velocity and robustness of superfluidity

Landau criterion. Superfluidity can be characterized by the existence of a finite critical velocity v_c, determined by the Landau criterion:

$$v_c = \min_{\boldsymbol{k}} \frac{\omega(\boldsymbol{k})}{|\boldsymbol{k}|} \quad \text{(appropriate branch)}. \tag{42}$$

There are two relevant low-energy branches: fermionic quasiparticles and bosonic phonons. The fermionic quasiparticles control the BCS regime v_c, while the bosonic phonons control the BEC regime.

Which excitation branch determines the critical velocity v_c

■ **BCS regime.** The fermionic quasiparticle dispersion is

$$E_k = \sqrt{(\epsilon_k - \mu)^2 + \Delta^2}, \qquad \epsilon_k = \frac{\hbar^2 k^2}{2m},$$

with the minimum gap Δ occurring at $k \simeq k_F$. Applying the Landau criterion to this branch gives

$$v_c^{(\text{fermionic})} = \min_k \frac{E_k}{\hbar k} \simeq \frac{\Delta}{\hbar k_F}.$$

By contrast, the phonon branch has dispersion $\omega = ck$ with

$$v_c^{(\text{bosonic})} = c \simeq \frac{v_F}{\sqrt{3}} = \frac{\hbar k_F}{\sqrt{3}m},$$

which is much larger than $\Delta/(\hbar k_F)$ in the weak-coupling BCS limit $\Delta \ll E_F$.
Therefore, the critical velocity is controlled by fermionic pair breaking,

$$v_c \simeq \frac{\Delta}{\hbar k_F}. \tag{43}$$

■ **BEC regime.** On the BEC side, fermionic excitations correspond to breaking tightly bound molecules.

$$v_c^{(\text{fermion})} = \min_k \frac{E_k}{\hbar k} = \frac{\sqrt{\xi_k^2 + \Delta^2}}{\hbar k_F} \simeq \frac{\epsilon_k + |\mu|}{\hbar k_F},$$

where we've used $\xi_k = \epsilon_k + |\mu| > |\mu| \gg \Delta$ in the BEC limit. Further simplify this equation and use some familiar result of $f(x) = x + \frac{1}{x}$:

$$\min\left(\frac{\epsilon_k + \mu}{\hbar k}\right) = \frac{\hbar}{2m} \cdot \min\left(\frac{k^2 + \frac{2m\mu}{\hbar^2}}{k}\right) = \frac{\hbar}{2m} \cdot 2\sqrt{\frac{2m\mu}{\hbar^2}}.$$

Then plug in $|\mu| = \frac{\hbar^2}{2ma_s^2}$ as the zeroth order approximation, we get:

$$v_c^{(\text{fermionic})} = \frac{\hbar}{ma_s}.$$

This candidate velocity then compete with the bosonic velocity given in (41).

$$\frac{v_c^{(\text{bosonic})}}{v_c^{(\text{fermionic})}} = \frac{\sqrt{4\pi\hbar^2 a_m n_m}}{2m} \cdot \frac{m a_s}{\hbar} \sim (k_F a_s)^{3/2} \ll 1 \Rightarrow v_c^{(\text{bosonic})} \ll v_c^{(\text{fermionic})}$$

So, the lowest branch is the phonon mode $\omega = ck$, and the Landau criterion yields

$$v_c \simeq c,$$

where c is the sound velocity of the molecular Bose–Einstein condensate.

Consequently, v_c typically reaches a maximum in an intermediate interaction regime, indicating the most robust superfluidity there.

5 Transition temperature

So far we have focused on the ground-state ($T = 0$) properties across the BCS–BEC crossover, such as the evolution of μ, Δ, and the nature of elementary excitations. At finite temperature, however, a qualitatively new question emerges: even if pairing correlations exist, the system is superfluid only when the pairs acquire *global phase coherence*. Therefore it is natural to study the transition temperature T_c separating a normal state (no long-range phase coherence) from a superfluid state (with broken $U(1)$ symmetry).

A key point in the crossover is that *pair formation* and *pair condensation* need not occur at the same temperature, especially on the BEC side.

5.1 Normal state vs superfluid state: what changes above T_c?

Mean-field Hamiltonian above T_c. Within the BCS mean-field framework, the superfluid order parameter is the pairing amplitude Δ. Above the transition temperature, the order parameter vanishes,

$$\Delta = 0 \qquad (T > T_c),$$

and the mean-field Hamiltonian reduces to that of a free Fermi gas:

$$\hat{H}_{\text{MF}}(T > T_c) = \sum_{\mathbf{k},\sigma} (\epsilon_{\mathbf{k}} - \mu) \hat{c}^\dagger_{\mathbf{k}\sigma} \hat{c}_{\mathbf{k}\sigma}, \tag{44}$$

whose free energy we denote by $\mathcal{F}_0$.

Minimal characterization: order parameter and phase coherence. The superfluid state is characterized by

$$\Delta \neq 0 \quad \Longleftrightarrow \quad \text{spontaneous breaking of global } U(1) \text{ (presence of phase coherence).}$$

The normal state has $\Delta = 0$, meaning the absence of long-range phase coherence. Importantly, $\Delta = 0$ does *not* necessarily imply the absence of pairing *correlations*: in the crossover (especially toward the BEC side), one may still have substantial short-range pairing ("preformed pairs") even though the system is not yet superfluid.

5.2 Landau expansion near a second-order transition

General structure. Assuming the transition is continuous (second order), the order parameter can be taken arbitrarily small near T_c. Thus the free energy admits an analytic expansion in powers of Δ:

$$\mathcal{F}(\Delta) = \mathcal{F}_0 + r(T,\mu)\,|\Delta|^2 + b(T,\mu)\,|\Delta|^4 + \cdots, \tag{45}$$

with $b > 0$ in the BCS mean-field setting. The sign of r determines the stable phase:

$$r > 0:\ \Delta = 0 \text{ (normal)}, \qquad r < 0:\ \Delta \neq 0 \text{ (superfluid)}, \qquad T_c:\ r(T_c,\mu) = 0.$$

Microscopic input (stated without proof). For a contact interaction treated in BCS mean-field, the quadratic coefficient can be written as

$$\frac{r(T,\mu)}{V} = -\frac{1}{V}\sum_{\boldsymbol{k}} \frac{1-2f(\xi_{\boldsymbol{k}})}{2\xi_{\boldsymbol{k}}} - \frac{1}{g}, \qquad \xi_{\boldsymbol{k}} \equiv \epsilon_{\boldsymbol{k}} - \mu, \tag{46}$$

where f is the Fermi distribution. A careful derivation of (46), and its renormalized form in terms of a_s, will be given in the next subsection.

5.3 Thouless criterion and the BCS limit

Thouless criterion as $r = 0$. The transition temperature is determined by

$$r(T_c,\mu) = 0, \tag{47}$$

which is the *Thouless criterion*. Equivalently, it says that the pairing susceptibility (the Cooper bubble) at zero center-of-mass momentum becomes singular, signaling an instability toward coherent pairing. In the BCS Mean-Field Hamiltonian case,

$$\frac{m}{4\pi\hbar^2 a_s} + \frac{1}{V}\sum_{\boldsymbol{k}} \left(\frac{1-2f(\xi_{\boldsymbol{k}})}{2\xi_{\boldsymbol{k}}} - \frac{1}{2\epsilon_{\boldsymbol{k}}} \right) = 0, \tag{48}$$

Deriving the Thouless criterion from the BCS mean-field Hamiltonian (quadratic order in Δ)

The weak-coupling BCS derivation of T_c is essentially a controlled *logarithmic* estimate near the Fermi surface, together with the statement that the coupling constant is a physical parameter (hence independent of temperature). The key steps can be organized as follows.

(i) Linearized gap equation / Thouless criterion at T_c. At $T = T_c$ the order parameter is infinitesimal, so $E_{\boldsymbol{k}} \to |\xi_{\boldsymbol{k}}|$ and the gap equation linearizes to

$$\frac{1}{|g|} = \frac{1}{V}\sum_{\boldsymbol{k}} \frac{1-2f(\xi_{\boldsymbol{k}})}{2\xi_{\boldsymbol{k}}} = \frac{1}{V}\sum_{\boldsymbol{k}} \frac{\tanh(\beta_c \xi_{\boldsymbol{k}}/2)}{2\xi_{\boldsymbol{k}}}, \qquad \xi_{\boldsymbol{k}} = \epsilon_{\boldsymbol{k}} - \mu,$$

which is equivalent to $r(T_c,\mu) = 0$ in the Landau expansion.

(ii) Why a cutoff Λ appears. The kernel behaves as $\tanh(\beta\xi/2)/\xi \simeq 1/\xi$ for $|\xi| \gg k_B T$, producing a logarithm from the energy shell $k_B T \ll |\xi| \ll \Lambda$. A high-energy cutoff is therefore unavoidable in the simplest "constant-g" model:

$$\int^{\infty} \frac{d\xi}{\xi} \text{ diverges.}$$

Physically, in conventional superconductors the effective attraction is mediated by phonons and is only operative within an energy window of order the Debye frequency, so one may take $\Lambda \sim \hbar\omega_D$. For cold atoms with contact interactions, the UV sensitivity is removed instead by renormalizing g in terms of a_s; the role of Λ is then merely intermediate bookkeeping.

(iii) Fermi-surface reduction. In weak coupling one has $\mu \simeq E_F$ and $\Lambda \ll \mu$ (e.g. $\omega_D \ll E_F$), so the density of states is approximately constant in the pairing window:

$$\frac{1}{V}\sum_{\boldsymbol{k}}(\cdots) \;\simeq\; N(0)\int_{-\Lambda}^{\Lambda} d\xi\,(\cdots), \qquad N(0) \equiv N(\epsilon)\big|_{\epsilon=\mu}.$$

Using that $\tanh(\beta\xi/2)/\xi$ is an even function gives

$$\frac{1}{|g|} \simeq N(0)\int_0^{\Lambda} d\xi\,\frac{\tanh(\beta_c\xi/2)}{\xi}.$$

The standard asymptotic evaluation for $\beta_c\Lambda \gg 1$ yields

$$\int_0^{\Lambda} d\xi\,\frac{\tanh(\beta_c\xi/2)}{\xi} = \ln\!\left(\frac{2e^{\gamma}}{\pi}\,\beta_c\Lambda\right) + O(e^{-\beta_c\Lambda}),$$

so that

$$\frac{1}{|g|} \simeq N(0)\ln\!\left(\frac{2e^{\gamma}}{\pi}\,\frac{\Lambda}{k_BT_c}\right).$$

(iv) The $T = 0$ gap equation and elimination of Λ. At $T = 0$ the BCS gap equation (in the same weak-coupling approximation) is [a]

$$\frac{1}{|g|} \simeq N(0)\int_0^{\Lambda}\frac{d\xi}{\sqrt{\xi^2+\Delta(0)^2}} = N(0)\,\operatorname{arsinh}\!\left(\frac{\Lambda}{\Delta(0)}\right) \simeq N(0)\ln\!\left(\frac{2\Lambda}{\Delta(0)}\right), \quad (\Lambda \gg \Delta(0)).$$

Since the left-hand side is the same physical coupling, the two equations must agree. Eliminating the unphysical cutoff Λ gives the universal BCS mean-field ratio

$$k_BT_c = \frac{e^{\gamma}}{\pi}\,\Delta(0), \qquad \Delta(0) \approx 1.764\,k_BT_c,$$

which is independent of the microscopic high-energy scale.

Takeaway. The cutoff Λ is introduced because (i) the pairing kernel produces a logarithm and (ii) the effective attraction has a finite energy range (e.g. ω_D), or equivalently because a constant contact coupling must be renormalized. Crucially, Λ cancels once we relate T_c to $\Delta(0)$, leaving a universal mean-field ratio.

[a] $\Delta(0)$ stands for "Δ at $T = 0$"

BCS-limit T_c and its relation to $\Delta(0)$. In the weak-coupling BCS limit, μ is only weakly renormalized, so we set $\mu \simeq E_F$ when solving $r(T_c, \mu) = 0$. This gives the standard exponentially small transition temperature,

$$k_BT_c = \frac{8e^{\gamma}}{\pi e^2}\,E_F\,\exp\!\left(\frac{\pi}{2k_Fa_s}\right). \tag{49}$$

BCS limit: a concrete computation of T_c from $r(T_c, \mu) = 0$

In weak coupling, the Thouless equation is dominated by states near the Fermi surface. Set $\mu \simeq E_F$ and approximate the density of states as a constant $N(0)$ in the relevant window. Then the (renormalized) Thouless equation is equivalent to

$$\frac{1}{|g|} \simeq N(0) \int_0^\Lambda d\xi \, \frac{\tanh\left(\beta_c \xi/2\right)}{\xi}, \qquad \beta_c \equiv \frac{1}{k_B T_c},$$

where Λ is a high-energy scale that drops out once we relate to the $T = 0$ gap. For $\Lambda \gg k_B T_c$, one uses the standard asymptotic evaluation

$$\int_0^\Lambda d\xi \, \frac{\tanh(\beta_c \xi/2)}{\xi} = \ln\left(\frac{2e^\gamma}{\pi} \beta_c \Lambda\right) + O\left(e^{-\beta_c \Lambda}\right),$$

hence

$$\frac{1}{|g|} \simeq N(0) \ln\left(\frac{2e^\gamma}{\pi} \frac{\Lambda}{k_B T_c}\right).$$

On the other hand, the $T = 0$ BCS gap equation in the same weak-coupling approximation gives

$$\frac{1}{|g|} \simeq N(0) \int_0^\Lambda d\xi \, \frac{1}{\sqrt{\xi^2 + \Delta(0)^2}} = N(0) \ln\left(\frac{2\Lambda}{\Delta(0)}\right).$$

Eliminating Λ between the two equations yields the universal mean-field ratio

$$k_B T_c = \frac{e^\gamma}{\pi} \Delta(0), \qquad \Delta(0) \approx 1.764 \, k_B T_c.$$

If one further inserts the standard weak-coupling result for the $T = 0$ gap in terms of a_s,

$$\Delta(0) = \frac{8}{e^2} E_F \exp\left(\frac{\pi}{2 k_F a_s}\right),$$

one obtains

$$k_B T_c = \frac{8 e^\gamma}{\pi e^2} E_F \, \exp\left(\frac{\pi}{2 k_F a_s}\right),$$

which matches the familiar BCS-limit expression.

Number conservation and μ. Beyond the strict BCS limit, μ varies substantially across the crossover and must be fixed by a number equation. If one insists on using the mean-field normal-state Hamiltonian above T_c, one would use

$$n_\sigma = n_{\text{free}} = \sum_k \frac{1}{e^{(\epsilon_k - \mu)/(k_B T)} + 1}, \tag{50}$$

together with the Thouless criterion (47).

5.4 Why mean-field T_c fails on the BEC side and what fixes it

Mean-field T_c becomes a *pair-formation* scale. Solving (50) and (47) yields a "T_c" that keeps increasing toward the BEC side. This behavior is unphysical: on the BEC side the relevant low-energy objects are bosonic molecules of density $n_m = n/2$, and their Bose–Einstein condensation

temperature is fixed by density and mass,

$$k_B T_{\mathrm{BEC}} \simeq 3.31 \, \frac{\hbar^2 n_m^{2/3}}{2m} \simeq 0.218 \, E_F. \tag{51}$$

The resolution is conceptual: the Thouless criterion by itself diagnoses the onset of strong pairing in the $\mathbf{q} = 0$ channel, i.e. a *pair-formation* (or pairing-instability) temperature. On the BEC side, pairs can form well above the temperature at which they acquire global phase coherence and Bose condense.

Noncondensed pairs and the corrected number equation. On the BEC side, a substantial fraction of particles resides in *finite center-of-mass momentum* pairs even above T_c. Counting only n_{free} therefore underestimates the total density. A minimal correction is to include the population of thermally excited (noncondensed) pairs,

$$n_\sigma = n_{\mathrm{free}} + n_{\mathrm{fluc}}, \tag{52}$$

where n_{fluc} can be estimated by Gaussian pair fluctuations (ladder summation / NSR). In the BCS limit, $n_{\mathrm{fluc}} \ll n_{\mathrm{free}}$ and the mean-field result survives; in the BEC limit, $n_{\mathrm{fluc}} \gg n_{\mathrm{free}}$ and the transition temperature reduces to the molecular condensation temperature (51).

Finite-T crossover in one sentence: mean-field Thouless criterion captures the onset of pairing, but the true superfluid T_c on the BEC side is controlled by Bose condensation of pairs, requiring noncondensed pairs in the number equation.

5.5 Computational approach: Gaussian fluctuations and NSR

Ladder diagrams and NSR approach. A simple approximation for n_{fluc} is to include Gaussian fluctuations, equivalently summing ladder diagrams in the pairing channel. While ladder summation is exact for the two-body problem, it becomes an approximation in the many-body setting. This is known as the Nozières–Schmitt-Rink (NSR) approach.

BCS and BEC limits within NSR. In the BCS limit at T_c,

$$n_{\mathrm{free}} \gg n_{\mathrm{fluc}}, \tag{53}$$

so pair fluctuations are insignificant and NSR recovers (**??**). In the BEC limit at T_c,

$$n_{\mathrm{fluc}} \gg n_{\mathrm{free}}, \tag{54}$$

and one can show approximately

$$n_{\mathrm{fluc}} = \frac{1}{V} \sum_{\boldsymbol{k}} \frac{1}{\exp\left[\left(\frac{\hbar^2 k^2}{4m} - \frac{\hbar^2}{m a_s^2} - 2\mu\right)/(k_B T)\right] - 1}. \tag{55}$$

As $2\mu \to -\hbar^2/(m a_s^2)$ in the BEC limit, $n \simeq n_{\mathrm{fluc}}$ reproduces the molecular BEC temperature (51).

Finite-T crossover: mean-field Thouless criterion captures the onset of pairing, but the true superfluid T_c on the BEC side requires counting noncondensed pairs, e.g. via Gaussian fluctuations / NSR.

6 The unitary regime

6.1 Definition and qualitative mean-field ground-state predictions

Unitary regime and scale invariance. The unitary regime is defined by

$$-\frac{1}{k_F a_s} \sim 0, \qquad a_s \to \infty, \tag{56}$$

realized by tuning near a Feshbach resonance. When a_s diverges, the system lacks any interaction-related length scale; the Fermi energy E_F becomes the only energy scale. This makes the unitary Fermi gas an example of a *scale-invariant* quantum many-body system.

Mean-field ground-state scaling. Since mean-field theory recovers correct physics in both BCS and BEC limits and the crossover is continuous, it can be expected to qualitatively capture some intermediate-regime ground-state trends. For instance, mean field predicts that at unitarity both μ/E_F and Δ/E_F are $O(1)$ constants, consistent with the statement that pairing and kinetic energies are comparable in scale.

6.2 Why theory is difficult: excitations and nonperturbativity

However, beyond the ground state physics, things are more complicated.

Superfluid state: fermions and bosons both matter. On the BCS side, low-energy physics is dominated by fermionic quasiparticles; on the BEC side, by bosonic phonons. At unitarity, both types of excitations are important and must be treated on equal footing.

Normal state: no small parameter. In the normal state, BCS side admits a perturbative parameter $k_F a_s$, and BEC side becomes a weakly interacting Bose gas of molecules after subtracting the binding energy, with $a_m^3 n_m$ as a small parameter. At unitarity the system is neither weakly interacting Fermi nor weakly interacting Bose: interaction energy is comparable to kinetic energy, making the problem intrinsically nonperturbative.

6.3 Symmetry, possible non-Fermi-liquid behavior, and holographic ideas

Schrödinger symmetry and open questions. It can be shown that the unitary Fermi gas possesses Schrödinger symmetry, a nonrelativistic analog of conformal symmetry (larger than Galilean symmetry). Due to strong interactions, it remains an open issue whether the normal state just above T_c is a Fermi liquid or a non-Fermi liquid, i.e., whether well-defined quasiparticles exist.

Holographic viscosity bound. A prediction inspired by holographic duality is a universal bound on the ratio of shear viscosity η to entropy density s:

$$\frac{\eta}{s} = \frac{\hbar}{4\pi k_B} \quad \text{(for theories with an Einstein-gravity dual)}, \tag{57}$$

and more generally it is conjectured that

$$\frac{\eta}{s} \geq \frac{\hbar}{4\pi k_B} \tag{58}$$

for all fluids. Experiments on unitary Fermi gases find that η/s approaches but does not violate this bound in the quantum-degenerate regime, and comparisons across different fluids suggest the bound is respected broadly. Notably, the unitary Fermi gas and quark–gluon plasma are among the systems closest to the bound, despite being realized at extremely different temperatures, both sharing the feature of strong interactions with interaction energy comparable to kinetic energy.

A Appendix: Solving the coupled gap and number equations for Δ and μ

In mean-field theory at $T = 0$, the superfluid state is determined by the *simultaneous* solution of the renormalized gap equation and the number equation:

$$-\frac{m}{4\pi\hbar^2 a_s} = \frac{1}{V}\sum_{\boldsymbol{k}}\left(\frac{1}{2E_k} - \frac{1}{2\epsilon_k}\right), \qquad E_k \equiv \sqrt{(\epsilon_k - \mu)^2 + \Delta^2}, \tag{59}$$

$$n_\sigma = \frac{1}{2V}\sum_{\boldsymbol{k}}\left(1 - \frac{\epsilon_k - \mu}{E_k}\right). \tag{60}$$

Here $\epsilon_k = \hbar^2 k^2/(2m)$, μ is the chemical potential, and Δ is the pairing gap. The physical density $n = 2n_\sigma$ is fixed, hence k_F and E_F are fixed by

$$n = \frac{k_F^3}{3\pi^2}, \qquad E_F = \frac{\hbar^2 k_F^2}{2m}. \tag{61}$$

A.1 Why the two equations are coupled

The gap equation alone does not fix Δ. Equation (59) depends on Δ and μ. If one were to hold μ fixed by hand (as in the weak-coupling BCS limit where $\mu \simeq E_F$), then the gap equation determines Δ. However, across the BCS–BEC crossover μ changes dramatically (from $\mu \simeq E_F$ to $\mu \simeq -E_b/2$), so one must determine μ self-consistently.

The number equation is the self-consistency condition. Equation (60) enforces particle-number conservation and fixes μ for a given Δ. Thus the coupled system {gap equation, number equation} closes the mean-field problem.

A.2 Dimensionless reduction: the only parameter is $-1/(k_F a_s)$

It is convenient to measure momenta in units of k_F and energies in units of E_F. Define

$$x \equiv \frac{k}{k_F}, \qquad \tilde{\mu} \equiv \frac{\mu}{E_F}, \qquad \tilde{\Delta} \equiv \frac{\Delta}{E_F}, \qquad \epsilon_k = E_F x^2. \tag{62}$$

Then

$$E_k = E_F\sqrt{(x^2 - \tilde{\mu})^2 + \tilde{\Delta}^2}. \tag{63}$$

Convert sums to integrals using

$$\frac{1}{V}\sum_{\boldsymbol{k}} \;\to\; \int \frac{d^3k}{(2\pi)^3} = \frac{k_F^3}{2\pi^2}\int_0^\infty dx\, x^2. \tag{64}$$

(i) The **number equation** becomes

$$\frac{n_\sigma}{k_F^3} = \frac{1}{2}\frac{1}{2\pi^2}\int_0^\infty dx\, x^2\left(1 - \frac{x^2 - \tilde{\mu}}{\sqrt{(x^2 - \tilde{\mu})^2 + \tilde{\Delta}^2}}\right). \tag{65}$$

Using $n_\sigma = k_F^3/(6\pi^2)$, this simplifies to the *dimensionless* constraint

$$\boxed{\int_0^\infty dx\, x^2\left(1 - \frac{x^2 - \tilde{\mu}}{\sqrt{(x^2 - \tilde{\mu})^2 + \tilde{\Delta}^2}}\right) = \frac{2}{3}.} \tag{66}$$

(ii) For the **gap equation**, write the left-hand side in terms of $-1/(k_F a_s)$:

$$-\frac{m}{4\pi\hbar^2 a_s} = -\frac{k_F}{4\pi}\frac{m}{\hbar^2}\frac{1}{k_F a_s} = -\frac{1}{4\pi}\frac{mk_F}{\hbar^2}\frac{1}{k_F a_s}. \tag{67}$$

On the right-hand side,

$$\frac{1}{V}\sum_{\boldsymbol{k}}\left(\frac{1}{2E_k} - \frac{1}{2\epsilon_k}\right) = \frac{k_F^3}{2\pi^2}\int_0^\infty dx\, x^2\left(\frac{1}{2E_F\sqrt{(x^2-\tilde{\mu})^2+\tilde{\Delta}^2}} - \frac{1}{2E_F x^2}\right). \tag{68}$$

Multiplying both sides by $4\pi^2 E_F/k_F^3$ and using $E_F = \hbar^2 k_F^2/(2m)$, one obtains the standard dimensionless gap equation

$$\boxed{-\frac{\pi}{2}\frac{1}{k_F a_s} = \int_0^\infty dx\left(\frac{x^2}{\sqrt{(x^2-\tilde{\mu})^2+\tilde{\Delta}^2}} - 1\right).} \tag{69}$$

Equations (66) and (69) show explicitly that the mean-field solution depends on a *single* tunable dimensionless interaction parameter $-1/(k_F a_s)$.

After rescaling by k_F and E_F, the coupled mean-field problem reduces to solving two dimensionless equations (66)–(69) for $(\tilde{\Delta}, \tilde{\mu})$ at a given $-1/(k_F a_s)$. No other microscopic parameter enters at this level.

A.3 Practical solution strategy – A numerical root finding problem

Define

$$F_1(\tilde{\Delta}, \tilde{\mu}; \lambda) \equiv \int_0^\infty dx\left(\frac{x^2}{\sqrt{(x^2-\tilde{\mu})^2+\tilde{\Delta}^2}} - 1\right) - \frac{\pi}{2}\lambda, \qquad \lambda \equiv -\frac{1}{k_F a_s}, \tag{70}$$

$$F_2(\tilde{\Delta}, \tilde{\mu}) \equiv \int_0^\infty dx\, x^2\left(1 - \frac{x^2-\tilde{\mu}}{\sqrt{(x^2-\tilde{\mu})^2+\tilde{\Delta}^2}}\right) - \frac{2}{3}. \tag{71}$$

Then the self-consistent mean-field solution is obtained from [8]

$$F_1(\tilde{\Delta}, \tilde{\mu}; \lambda) = 0, \qquad F_2(\tilde{\Delta}, \tilde{\mu}) = 0. \tag{72}$$

This is a standard two-variable nonlinear root-finding problem. We can design a numerical method to robustly locate the simultaneous root $(\tilde{\Delta}, \tilde{\mu})$ for a fixed coupling λ.

(i) Lower limit $x \to 0$**.** Fix $(\tilde{\Delta}, \tilde{\mu})$ with $\tilde{\Delta} > 0$. As $x \to 0$,

$$\sqrt{(x^2-\tilde{\mu})^2+\tilde{\Delta}^2} = \sqrt{\tilde{\mu}^2+\tilde{\Delta}^2} + O(x^2),$$

hence

$$\frac{x^2}{\sqrt{(x^2-\tilde{\mu})^2+\tilde{\Delta}^2}} - 1 = -1 + \frac{x^2}{\sqrt{\tilde{\mu}^2+\tilde{\Delta}^2}} + O(x^4), \qquad (x \to 0),$$

[8] $F_1 \sim$ gap eq. $\quad F_2 \sim$ number eq.

which is integrable at the origin. Likewise,

$$x^2\left(1-\frac{x^2-\tilde{\mu}}{\sqrt{(x^2-\tilde{\mu})^2+\tilde{\Delta}^2}}\right)=x^2\left(1+\frac{\tilde{\mu}}{\sqrt{\tilde{\mu}^2+\tilde{\Delta}^2}}\right)+O(x^4),\qquad (x\to 0),$$

so the F_2 integrand vanishes as $O(x^2)$. Therefore the lower limit causes no singular behavior and standard quadrature applies.

(ii) Upper limit $x\to\infty$ and truncation. For $x\gg 1$,

$$\sqrt{(x^2-\tilde{\mu})^2+\tilde{\Delta}^2}=(x^2-\tilde{\mu})\left[1+\frac{\tilde{\Delta}^2}{2(x^2-\tilde{\mu})^2}+O(x^{-8})\right].$$

It follows that

$$\frac{x^2}{\sqrt{(x^2-\tilde{\mu})^2+\tilde{\Delta}^2}}-1=\frac{\tilde{\mu}}{x^2}+O(x^{-4}),\qquad (x\to\infty),$$

and

$$x^2\left(1-\frac{x^2-\tilde{\mu}}{\sqrt{(x^2-\tilde{\mu})^2+\tilde{\Delta}^2}}\right)=\frac{\tilde{\Delta}^2}{2x^2}+O(x^{-4}),\qquad (x\to\infty),$$

so both integrands decay as $O(x^{-2})$. Hence the improper integrals may be safely truncated to $[0,x_{\max}]$ with a large cutoff $x_{\max}$, and convergence can be checked by increasing $x_{\max}$ and compare the results.

(iii) Two-dimensional scan at fixed λ. For a given λ, one performs a coarse scan over a rectangular domain

$$\tilde{\Delta}\in[\Delta_{\min},\Delta_{\max}],\qquad \tilde{\mu}\in[\mu_{\min},\mu_{\max}],$$

evaluates F_1 and F_2 on a grid (with the integrals truncated at $x_{\max}$), and identifies the intersection(s) of the zero-level sets $F_1=0$ and $F_2=0$ as candidate solutions. A local two-variable solver (e.g. Newton or quasi-Newton) can then be used to refine the candidates, yielding the self-consistent mean-field solution $(\tilde{\Delta},\tilde{\mu})$ at that λ.

The numerical solutions $\tilde{\Delta}(\lambda)$ and $\tilde{\mu}(\lambda)$ are summarized in Fig. 5.

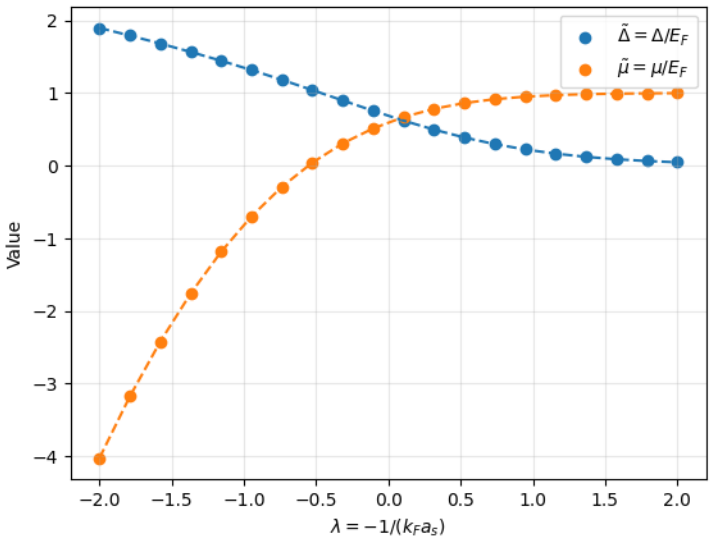

Figure 5: Behaviors of $\tilde{\Delta}(\lambda)$ and $\tilde{\mu}(\lambda)$

As $\lambda \to +\infty$, we find $\tilde{\Delta} \to 0$ while $\tilde{\mu} \to 1$. This is the weak-coupling BCS regime: the interaction is attractive ($a_s < 0$) and weak ($|k_F a_s| \ll 1$). In this limit the gap Δ is exponentially small in terms of $-\lambda$ (as we will show later), and the chemical potential remains close to the Fermi energy, $\mu \simeq E_F$, reflecting a fermionic system with a well-defined Fermi surface.

On the other hand, as $\lambda \to +\infty$ (weak repulsion on the BEC side, $a_s > 0$ and $|k_F a_s| \ll 1$), $\tilde{\mu}$ becomes negative while $\tilde{\Delta}$ grows large. The negative chemical potential indicates that the relevant low-energy degrees of freedom are no longer fermionic quasiparticles near a Fermi surface, but rather tightly bound bosonic molecules. In this BEC regime, Δ should not be interpreted as a fermionic excitation gap controlling the low-energy physics; instead, the low-energy sector is governed by the dynamics of these composite bosons.

A.4 The BCS limit expansion

We consider the BCS limit behavior, *i.e.* the region where $\lambda = -1/k_F a_s \gg 1$, $\Delta \to 0$ and $\mu \to E_F$. The key idea is to extract the leading-order behavior of Δ and μ with respect to their dependence on λ by solving the equations iteratively, order by order. We start from the zeroth order $\tilde{\mu} = 1$ and $\tilde{\Delta} = 0$.

A.4.1 $\tilde{\Delta}$ as a function of λ

To estimate the integration in the gap equation (70), we set $\tilde{\mu} = 1$ and define:

$$I(\tilde{\Delta}) \equiv \int_0^\infty dx \left(\frac{x^2}{\sqrt{(x^2-1)^2 + \tilde{\Delta}^2}} - 1 \right).$$

As a a priori knowledge, we know that $\tilde{\Delta} \to 0$. So, in the $x \in [1-\delta, 1+\delta]$ region, the integral exhibits a divergence that depends on $\tilde{\Delta}$.

Fix a $\delta \in (0,1)$ independent of $\tilde{\Delta}$ and split

$$I(\tilde{\Delta}) = I_<(\tilde{\Delta}) + I_{\text{mid}}(\tilde{\Delta}) + I_>(\tilde{\Delta}), \quad I_< \equiv \int_0^{1-\delta}, \; I_{\text{mid}} \equiv \int_{1-\delta}^{1+\delta}, \; I_> \equiv \int_{1+\delta}^{\infty}.$$

(1) Outer regions (finite as $\tilde{\Delta} \to 0$). For fixed δ, we may set $\tilde{\Delta} = 0$ in $I_<$ and $I_>$.

For $x < 1$, $\sqrt{(x^2-1)^2} = 1 - x^2$, hence

$$\frac{x^2}{|x^2-1|} - 1 = \frac{x^2}{1-x^2} - 1 = \frac{1}{1-x^2} - 2.$$

For $x > 1$, $\sqrt{(x^2-1)^2} = x^2 - 1$, hence

$$\frac{x^2}{|x^2-1|} - 1 = \frac{x^2}{x^2-1} - 1 = \frac{1}{x^2-1}.$$

Therefore

$$I_<(0) = \int_0^{1-\delta} \left(\frac{1}{1-x^2} - 2 \right) dx = \frac{1}{2} \ln \frac{2-\delta}{\delta} - 2(1-\delta),$$

$$I_>(0) = \int_{1+\delta}^{\infty} \frac{dx}{x^2-1} = \frac{1}{2} \ln \frac{2+\delta}{\delta}.$$

So the outer contribution is

$$I_<(0) + I_>(0) = \frac{1}{2} \ln \frac{4-\delta^2}{\delta^2} - 2 + 2\delta. \tag{73}$$

(2) Near-shell region (logarithm + finite matching). In the middle interval $x \in [1-\delta, 1+\delta]$, set $t = x^2 - 1$. Then $x = \sqrt{1+t}$ and

$$dx = \frac{dt}{2\sqrt{1+t}}, \qquad t_\pm = (1\pm\delta)^2 - 1 = \pm 2\delta + \delta^2.$$

Therefore,

$$I_{\text{mid}}(\tilde{\Delta}) = \int_{1-\delta}^{1+\delta} dx \left(\frac{x^2}{\sqrt{(x^2-1)^2 + \tilde{\Delta}^2}} - 1 \right) = \frac{1}{2} \int_{t_-}^{t_+} dt \left(\frac{\sqrt{1+t}}{\sqrt{t^2+\tilde{\Delta}^2}} - \frac{1}{\sqrt{1+t}} \right). \tag{74}$$

Now insert and subtract the singular kernel $1/\sqrt{t^2+\tilde{\Delta}^2}$ and also add/subtract 1:

$$I_{\text{mid}}(\tilde{\Delta}) = \frac{1}{2} \int_{t_-}^{t_+} dt \left[\left(\frac{1}{\sqrt{t^2+\tilde{\Delta}^2}} - 1 \right) + \frac{\sqrt{1+t}-1}{\sqrt{t^2+\tilde{\Delta}^2}} - \left(\frac{1}{\sqrt{1+t}} - 1 \right) \right]. \tag{75}$$

After a long and technical calculation, one reach the result

$$I_{\text{mid}}(\tilde{\Delta}) = -\ln\tilde{\Delta} + \frac{1}{2}\ln\!\left(4\delta^2(4-\delta^2)\right) - 2\delta + \ln\frac{4}{4-\delta^2} + o(1), \qquad (\tilde{\Delta}\to 0), \tag{76}$$

Detailed Evaluation of $I_{\text{mid}}(\tilde{\Delta})$

We evaluate the three terms in (75).

(a) The last term vanishes exactly. Indeed,

$$\int \left(\frac{1}{\sqrt{1+t}} - 1 \right) dt = 2\sqrt{1+t} - t,$$

so

$$-\frac{1}{2} \int_{t_-}^{t_+} \left(\frac{1}{\sqrt{1+t}} - 1 \right) dt = -\frac{1}{2} \Big[2\sqrt{1+t} - t \Big]_{t_-}^{t_+}.$$

Using $\sqrt{1+t_+} = 1+\delta$ and $\sqrt{1+t_-} = 1-\delta$,

$$2\sqrt{1+t_+} - t_+ = 2(1+\delta) - (2\delta+\delta^2) = 2-\delta^2, \qquad 2\sqrt{1+t_-} - t_- = 2(1-\delta) - (-2\delta+\delta^2) = 2-\delta^2,$$

hence the difference is zero and the last term indeed *vanishes exactly*.

(b) The middle term is finite and can be evaluated at $\tilde{\Delta} = 0$. Since $\sqrt{1+t} - 1 = O(t)$ as $t \to 0$, the integrand $\left(\sqrt{1+t}-1\right)/\sqrt{t^2+\tilde{\Delta}^2}$ is integrable on $[t_-, t_+]$ uniformly for small $\tilde{\Delta}$; therefore

$$\frac{1}{2} \int_{t_-}^{t_+} dt \, \frac{\sqrt{1+t}-1}{\sqrt{t^2+\tilde{\Delta}^2}} = \frac{1}{2} \int_{t_-}^{t_+} dt \, \frac{\sqrt{1+t}-1}{|t|} + o(1), \qquad (\tilde{\Delta}\to 0).$$

To compute the $\tilde{\Delta} = 0$ value, split at $t = 0$ because of $|t|$:

$$\frac{1}{2} \int_{t_-}^{t_+} dt \, \frac{\sqrt{1+t}-1}{|t|} = \frac{1}{2} \left[\int_{t_-}^{0} dt \, \frac{\sqrt{1+t}-1}{-t} + \int_{0}^{t_+} dt \, \frac{\sqrt{1+t}-1}{t} \right].$$

In each integral substitute $u = \sqrt{1+t}$ so that $t = u^2 - 1$ and $dt = 2u\,du$. For $t \in [0, t_+]$, $u \in [1, 1+\delta]$, and

$$\frac{\sqrt{1+t}-1}{t}\, dt = \frac{u-1}{u^2-1}\, 2u\, du = \frac{2u}{u+1}\, du,$$

hence

$$\int_0^{t_+} dt\,\frac{\sqrt{1+t}-1}{t} = \int_1^{1+\delta} \frac{2u}{u+1}\,du = 2\Big[u-\ln(u+1)\Big]_1^{1+\delta} = 2\left(\delta + \ln\frac{2}{2+\delta}\right).$$

For $t \in [t_-, 0]$, $u \in [1-\delta, 1]$, and

$$\frac{\sqrt{1+t}-1}{-t}\,dt = \frac{u-1}{1-u^2}\,2u\,du = -\frac{2u}{u+1}\,du,$$

thus

$$\int_{t_-}^{0} dt\,\frac{\sqrt{1+t}-1}{-t} = \int_{1-\delta}^{1}\left(-\frac{2u}{u+1}\right)du = -2\Big[u-\ln(u+1)\Big]_{1-\delta}^{1} = 2\left(\delta + \ln\frac{2}{2-\delta}\right).$$

Adding the two pieces and multiplying by $1/2$ gives

$$\frac{1}{2}\int_{t_-}^{t_+} dt\,\frac{\sqrt{1+t}-1}{|t|} = \ln\frac{4}{4-\delta^2}. \tag{77}$$

(c) The singular term gives $-\ln\tilde{\Delta}$ plus a cutoff-dependent constant. Compute explicitly

$$\frac{1}{2}\int_{t_-}^{t_+}\left(\frac{1}{\sqrt{t^2+\tilde{\Delta}^2}}-1\right)dt = \frac{1}{2}\Big[\operatorname{asinh}(t/\tilde{\Delta})\Big]_{t_-}^{t_+} - \frac{t_+-t_-}{2}. \tag{78}$$

As $\tilde{\Delta}\to 0$, we have $t_+/\tilde{\Delta}\to+\infty$ and $t_-/\tilde{\Delta}\to-\infty$, and

$$\operatorname{asinh} z = \ln(2z) + o(1) \quad (z\to+\infty), \qquad \operatorname{asinh} z = -\ln(2|z|) + o(1) \quad (z\to-\infty).$$

Therefore,

$$\begin{aligned}\frac{1}{2}\Big[\operatorname{asinh}(t/\tilde{\Delta})\Big]_{t_-}^{t_+} &= \frac{1}{2}\left(\ln\frac{2t_+}{\tilde{\Delta}} + \ln\frac{2|t_-|}{\tilde{\Delta}}\right) + o(1)\\ &= -\ln\tilde{\Delta} + \frac{1}{2}\ln\Big(4t_+|t_-|\Big) + o(1), \qquad (\tilde{\Delta}\to 0).\end{aligned}$$

Noting $t_+|t_-| = (2\delta+\delta^2)(2\delta-\delta^2) = \delta^2(4-\delta^2)$ and

$$\frac{t_+-t_-}{2} = \frac{(2\delta+\delta^2)-(-2\delta+\delta^2)}{2} = 2\delta,$$

Eq. (78) becomes

$$\frac{1}{2}\int_{t_-}^{t_+}\left(\frac{1}{\sqrt{t^2+\tilde{\Delta}^2}}-1\right)dt = -\ln\tilde{\Delta} + \frac{1}{2}\ln\Big(4\delta^2(4-\delta^2)\Big) - 2\delta + o(1). \tag{79}$$

(d) Combine the pieces. Using (75), the exact cancellation of the last term, and (77)–(79), we obtain

$$I_{\mathrm{mid}}(\tilde{\Delta}) = -\ln\tilde{\Delta} + \frac{1}{2}\ln\Big(4\delta^2(4-\delta^2)\Big) - 2\delta + \ln\frac{4}{4-\delta^2} + o(1), \qquad (\tilde{\Delta}\to 0),$$

which is the desired near-shell contribution including the logarithm and the finite matching terms.

(3) Add all pieces and cancel δ-dependence. Summing (73) with (76), all δ-dependent terms cancel, and we arrive at the $\tilde{\Delta} \to 0$ asymptotics Collecting the contributions from the outer regions and the near-shell region, we obtain

$$I(\tilde{\Delta}) = \underbrace{\left[\frac{1}{2}\ln\frac{4-\delta^2}{\delta^2} - 2 + 2\delta\right]}_{\text{outer regions}} + \underbrace{\left[-\ln\tilde{\Delta} + \frac{1}{2}\ln\Big(4\delta^2(4-\delta^2)\Big) - 2\delta + \ln\frac{4}{4-\delta^2}\right]}_{\text{near-shell region}} + o(1). \tag{80}$$

All δ-dependent terms cancel identically, leaving

$$I(\tilde{\Delta}) = -\ln\tilde{\Delta} + \ln 8 - 2 + o(1) = \ln\left(\frac{8}{e^2\,\tilde{\Delta}}\right) + o(1), \qquad (\tilde{\Delta} \to 0). \tag{81}$$

Substituting the gap equation $F_1 = 0$, i.e. $I(\tilde{\Delta}) = \frac{\pi}{2}\lambda$, we immediately obtain

$$\tilde{\Delta} = \frac{8}{e^2}\, e^{-\frac{\pi}{2}\lambda}.$$

Restoring dimensions ($\Delta = \tilde{\Delta}E_F$ and $\lambda = -1/(k_F a_s)$) yields

$$\Delta = \frac{8E_F}{e^2}\exp\left\{\frac{\pi}{2k_F a_s}\right\}, \tag{82}$$

which reproduces the standard weak-coupling BCS result (20).

A.4.2 $\tilde{\mu}$ as a function of λ

We can also evaluate the behavior of $\tilde{\mu}$ in terms of $\tilde{\Delta}$ using the number equation $F_2 = 0$. We have $\tilde{\Delta} \ll 1$ and $\tilde{\mu} = 1 + O(\tilde{\Delta})$. Write

$$\tilde{\mu} = 1 + \delta\tilde{\mu}, \qquad \delta\tilde{\mu} = O(\tilde{\Delta}^2),$$

and expand the number equation $F_2(\tilde{\Delta}, \tilde{\mu}) = 0$ around $(\tilde{\Delta}, \tilde{\mu}) = (0, 1)$. Since F_2 is an even function of $\tilde{\Delta}$, the first correction starts at $O(\tilde{\Delta}^2)$:

$$0 = F_2(\tilde{\Delta}, 1 + \delta\tilde{\mu}) = F_2(0,1) + \left.\frac{\partial F_2}{\partial\tilde{\mu}}\right|_{(0,1)}\delta\tilde{\mu} + \frac{1}{2}\left.\frac{\partial^2 F_2}{\partial\tilde{\Delta}^2}\right|_{(0,1)}\tilde{\Delta}^2 + o(\tilde{\Delta}^2). \tag{83}$$

We already know $F_2(0,1) = 0$. Moreover, from the $\tilde{\Delta} = 0$ evaluation

$$F_2(0,\tilde{\mu}) = \frac{2}{3}\tilde{\mu}^{3/2} - \frac{2}{3},$$

it follows immediately that

$$\left.\frac{\partial F_2}{\partial\tilde{\mu}}\right|_{(0,1)} = \left.\frac{d}{d\tilde{\mu}}\left(\frac{2}{3}\tilde{\mu}^{3/2} - \frac{2}{3}\right)\right|_{\tilde{\mu}=1} = 1.$$

The remaining task is to extract the coefficient of $\tilde{\Delta}^2$. A careful near-shell/outer-region matching (analogous to the derivation of the BCS gap prefactor) gives the finite second derivative

$$\frac{1}{2}\left.\frac{\partial^2 F_2}{\partial\tilde{\Delta}^2}\right|_{(0,1)} = 2.$$

Substituting these results into (83) yields

$$0 = \delta\tilde{\mu} + 2\tilde{\Delta}^2 + o(\tilde{\Delta}^2), \qquad \Longrightarrow \qquad \tilde{\mu} = 1 - 2\tilde{\Delta}^2 + o(\tilde{\Delta}^2).$$

In terms of dimensionful quantities ($\mu = E_F\tilde{\mu}$ and $\Delta = E_F\tilde{\Delta}$), this becomes

$$\mu = E_F - \frac{2\Delta^2}{E_F} + o\left(\frac{\Delta^2}{E_F}\right),$$

so the deviation of μ from E_F is $O(\Delta^2/E_F)$, i.e. exponentially small in λ via $\Delta(\lambda)$.

A.5 The BEC limit expansion

We now consider the BEC limit of the mean-field equations, *i.e.* the regime $\lambda = -\frac{1}{k_F a_s} \ll -1$, corresponding to weak attraction with positive scattering length $a_s > 0$ and $k_F a_s \ll 1$. From the numerical results in 5, this limit is characterized by$\tilde{\mu} \to -\infty, \tilde{\Delta} \to +\infty$.

The essential physics of the BEC limit is that the fermionic system continuously evolves into a dilute gas of tightly bound diatomic molecules. From the underlying two-body problem in vacuum, one knows that for $a_s > 0$ a bound state exists with binding energy $E_b = \frac{\hbar^2}{m a_s^2}$. In a many-body system at low density, the chemical potential of a single fermion must therefore approach $\mu \simeq -\frac{E_b}{2}$, up to interaction-induced corrections between molecules. In dimensionless form, this implies the scaling

$$\tilde{\mu} = \frac{\mu}{E_F} \sim -\frac{1}{(k_F a_s)^2}, \qquad (k_F a_s \ll 1). \tag{84}$$

We consider the excitation energy give by BCS mean field theory.

$$E_k = \sqrt{(\epsilon_k - \mu)^2 + \Delta^2} = \sqrt{(\epsilon_k + |\mu|)^2 + \Delta^2}. \tag{85}$$

Since the chemical potential is negative, the minimal fermionic quasiparticle excitation is achieved at $k = 0$:

$$\min_k E_k = \sqrt{\mu^2 + \Delta^2} \sim \max(\mu, \Delta), \tag{86}$$

which is controlled by the bigger one of μ and Δ. Intuitively, the lowest excitation energy corresponds to breaking the binding of a fermionic pair, *i.e.* $\min_k E_k \sim \mu$. If Δ were comparable to or larger than $|\mu|$, the lowest excitation energy is described by the momentum paring process Δ, leading to a clear physical inconsistency. Thus, on physical grounds alone, one expects

$$\Delta \ll |\mu| \qquad \text{in the BEC limit.}$$

This expectation is directly confirmed by the numerical solution of the coupled equations, as shown in Fig. 6. From the numerical data one finds that, as $k_F a_s \to 0^+$, $\frac{\Delta}{|\mu|} \sim (k_F a_s)^{3/2}$, which vanishes algebraically. Therefore, in the BEC limit $k_F a_s \ll 1$, it is self-consistent to treat $\Delta/|\mu|$ as a small parameter and perform controlled expansions.

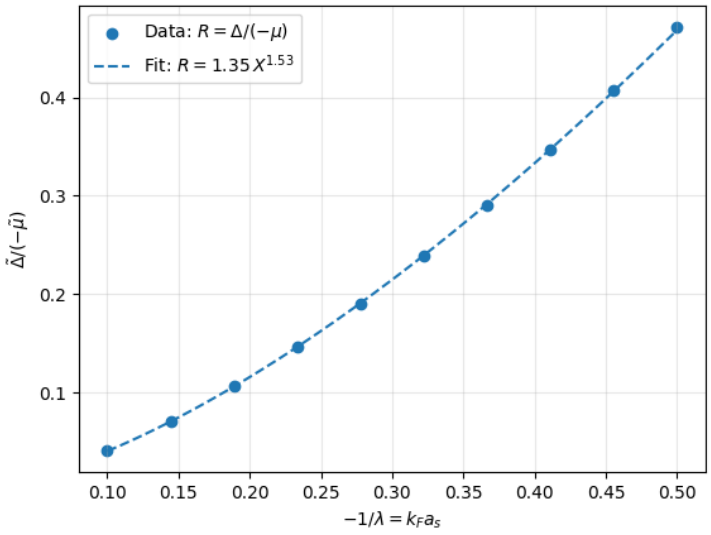

Figure 6: Numerical result of $\tilde{\Delta}/|\tilde{\mu}|$

■ **Number equation: $\tilde{\Delta}$–$\tilde{\mu}$ scaling, and self-consistency of small $\tilde{\Delta}$ expansion.**

We first evaluate the number equation,

$$F_2(\tilde{\Delta},\tilde{\mu}) \equiv \int_0^\infty dx\, x^2 \left(1 - \frac{x^2-\tilde{\mu}}{\sqrt{(x^2-\tilde{\mu})^2+\tilde{\Delta}^2}}\right) - \frac{2}{3}. \tag{87}$$

In the BEC limit $a_s > 0$ and $k_F a_s \ll 1$, the solution satisfies $\tilde{\mu} \to -\infty$. Set $u = -\tilde{\mu} > 0$ and write

$$E(x) \equiv \sqrt{(x^2-\tilde{\mu})^2+\tilde{\Delta}^2} = \sqrt{(x^2+u)^2+\tilde{\Delta}^2} = (x^2+u)\sqrt{1+\frac{\tilde{\Delta}^2}{(x^2+u)^2}}.$$

Assuming $\tilde{\Delta}/u \ll 1$(to be checked *a posteriori*), and thus $\tilde{\Delta}^2/(x^2+u)^2 \ll 1$, we expand

$$\frac{x^2-\tilde{\mu}}{\sqrt{(x^2-\tilde{\mu})^2+\tilde{\Delta}^2}} = \frac{x^2+u}{E(x)} = \left(1+\frac{\tilde{\Delta}^2}{(x^2+u)^2}\right)^{-1/2} = 1 - \frac{\tilde{\Delta}^2}{2(x^2+u)^2} + O\!\left(\frac{\tilde{\Delta}^4}{(x^2+u)^4}\right).$$

Hence the integrand in F_2 becomes

$$x^2\left(1-\frac{x^2-\tilde{\mu}}{E(x)}\right) = \frac{\tilde{\Delta}^2}{2}\frac{x^2}{(x^2+u)^2} + O\!\left(\tilde{\Delta}^4\frac{x^2}{(x^2+u)^4}\right).$$

Keeping only the leading term, the gap equation $F_2 = 0$ gives

$$\frac{\tilde{\Delta}^2}{2}\int_0^\infty dx\,\frac{x^2}{(x^2+u)^2} = \frac{2}{3}.$$

Evaluate the integral by $x = \sqrt{u}\,y$:

$$\int_0^\infty dx\,\frac{x^2}{(x^2+u)^2} = \frac{1}{\sqrt{u}}\int_0^\infty dy\,\frac{y^2}{(1+y^2)^2} = \frac{1}{\sqrt{u}}\cdot\frac{\pi}{4},$$

where $\int_0^\infty dy\,\frac{y^2}{(1+y^2)^2} = \frac{\pi}{4}$ [9]. Therefore,

$$\tilde{\Delta}^2 = \frac{16}{3\pi}\sqrt{u}, \qquad \text{i.e.} \qquad \tilde{\Delta} \sim u^{1/4}.$$

This immediately implies the hierarchy

$$\frac{\tilde{\Delta}}{u} \sim u^{-3/4} \ll 1 \qquad (u \to \infty),$$

which is precisely the self-consistency check of the small $\tilde{\Delta}/u$ expansion used above.

■ **Gap equation: zeroth order in $\tilde{\Delta}$.**

We then evaluate the gap equation,

$$F_1(\tilde{\Delta},\tilde{\mu};\lambda) \equiv \int_0^\infty dx\left(\frac{x^2}{\sqrt{(x^2-\tilde{\mu})^2+\tilde{\Delta}^2}} - 1\right) - \frac{\pi}{2}\lambda, \qquad \lambda \equiv -\frac{1}{k_F a_s}, \tag{88}$$

[9] Let, for example, $y = \tan\theta$

At zeroth order, set $\tilde{\Delta} = 0$. Since $u > 0$, we have $E(x) = |x^2 + u| = x^2 + u$, and the integrand in F_1 simplifies to

$$\frac{x^2}{E(x)} - 1 = \frac{x^2}{x^2+u} - 1 = -\frac{u}{x^2+u}.$$

Thus

$$\int_0^\infty dx \left(\frac{x^2}{\sqrt{(x^2+u)^2}} - 1 \right) = -u \int_0^\infty \frac{dx}{x^2+u} = -u \cdot \frac{1}{\sqrt{u}} \int_0^\infty \frac{dy}{1+y^2} = -\frac{\pi}{2}\sqrt{u}.$$

Imposing $F_1 = 0$ then yields

$$-\frac{\pi}{2}\sqrt{u} - \frac{\pi}{2}\lambda = 0 \qquad \Longrightarrow \qquad \sqrt{u} = -\lambda, \qquad u = \lambda^2,$$

so the leading BEC behavior is

$$\tilde{\mu} = -u \simeq -\lambda^2 = -\frac{1}{(k_F a_s)^2}. \tag{89}$$

■ **Gap equation : first order correction in $\tilde{\Delta}$.**

To include the leading $\tilde{\Delta}$-dependence, expand

$$\frac{1}{E(x)} = \frac{1}{x^2+u}\left(1 + \frac{\tilde{\Delta}^2}{(x^2+u)^2}\right)^{-1/2} = \frac{1}{x^2+u}\left[1 - \frac{\tilde{\Delta}^2}{2(x^2+u)^2} + O\left(\frac{\tilde{\Delta}^4}{(x^2+u)^4}\right)\right].$$

Then

$$\frac{x^2}{E(x)} - 1 = \frac{x^2}{x^2+u} - 1 - \frac{\tilde{\Delta}^2}{2}\frac{x^2}{(x^2+u)^3} + O\left(\frac{\tilde{\Delta}^4}{(x^2+u)^5}\right) = -\frac{u}{x^2+u} - \frac{\tilde{\Delta}^2}{2}\frac{x^2}{(x^2+u)^3} + \cdots.$$

Integrating the correction term (again $x = \sqrt{u}\, y$),

$$\int_0^\infty dx \, \frac{x^2}{(x^2+u)^3} = \frac{1}{u^{3/2}} \int_0^\infty dy \, \frac{y^2}{(1+y^2)^3} = \frac{1}{u^{3/2}} \cdot \frac{\pi}{16},$$

where $\int_0^\infty dy \, \frac{y^2}{(1+y^2)^3} = \frac{\pi}{16}$ [10]. Hence, up to $O(\tilde{\Delta}^2)$,

$$\int_0^\infty dx \left(\frac{x^2}{E(x)} - 1 \right) = -\frac{\pi}{2}\sqrt{u} - \frac{\tilde{\Delta}^2}{2} \cdot \frac{\pi}{16u^{3/2}} + O\left(\frac{\tilde{\Delta}^4}{u^{7/2}}\right) = -\frac{\pi}{2}\sqrt{u} - \frac{\pi}{32}\frac{\tilde{\Delta}^2}{u^{3/2}} + \cdots.$$

Imposing $F_1 = 0$ gives the corrected relation

$$-\sqrt{u} - \frac{1}{16}\frac{\tilde{\Delta}^2}{u^{3/2}} = \lambda + O\left(\frac{\tilde{\Delta}^4}{u^{7/2}}\right).$$

Using the leading-order number-equation result $\tilde{\Delta}^2 = \frac{16}{3\pi}\sqrt{u}$ and $\sqrt{u} \simeq -\lambda$, one finds the next correction

$$u = \lambda^2 + \frac{2}{3\pi}\frac{1}{\lambda} + o\left(\frac{1}{\lambda}\right), \qquad (\lambda \to -\infty),$$

equivalently

$$\begin{aligned} \tilde{\mu} = -u &= -\lambda^2 - \frac{2}{3\pi}\frac{1}{\lambda} + o\left(\frac{1}{\lambda}\right) \\ &= -\frac{1}{(k_F a_s)^2} + \frac{2}{3\pi}(k_F a_s) + \cdots. \end{aligned} \tag{90}$$

[10] Again, $y = \tan\theta$)

Summary. In the BEC regime $k_F a_s \ll 1$, the mean-field equations correctly reproduce the two-body binding physics through $\mu \simeq -E_b/2$, while the pairing gap grows more slowly and does not control the low-energy spectrum. The controlled hierarchy $\Delta \ll |\mu|$ justifies the asymptotic expansion and provides a clear physical interpretation of the BEC limit as a dilute Bose gas of tightly bound fermion pairs.

A.6 Physical interpretation of the self-consistent solution

What $\tilde{\mu}$ encodes. The chemical potential μ measures the energy cost of adding a fermion. In the BCS regime, fermions are added near a Fermi surface, hence $\mu \sim E_F$. In the BEC regime, adding two fermions primarily creates a molecule with binding energy $-\hbar^2/(ma_s^2)$, hence $\mu \sim -\hbar^2/(2ma_s^2)$.

What $\tilde{\Delta}$ encodes. The parameter Δ sets the scale for pair correlations and the fermionic excitation gap.

The coupled gap+number equations implement the essential crossover physics at mean-field level: μ evolves from $\approx E_F$ (BCS) to $\approx -\hbar^2/(2ma_s^2)$ (BEC), while Δ evolves from exponentially small to parametrically larger, with both determined self-consistently by a single control parameter $-1/(k_F a_s)$.